Electronic Supplementary Material (ESI) for Journal of Materials Chemistry C.
This journal is © The Royal Society of Chemistry 2023

Supporting Information
for
Elucidating the superexchange mechanisms in magnetic coordination polymer $[Co(HCOO)_2(H_2O)_2]_\infty$ through chemical bonding analysis

Thomas Bjørn Egede Grønbech,[1] Lennard Krause,[1] Davide Ceresoli,[2*] Bo Brummerstedt Iversen[1*]

[1]Center for Integrated Materials Research, Department of Chemistry, and iNANO, Aarhus University, Langelandsgade 140, DK-8000 Aarhus C, Denmark

[2]Istituto di Scienze e Tecnologie Chimiche "Giulio Natta" (SCITEC), National Research Council (CNR), I-20133, Milano, Italy

*Corresponding authors: davide.ceresoli@cnr.it, bo@chem.au.dk

1 THEORETICAL MODEL

The employed spin Hamiltonian is as follows using the broken symmetry method[1] to generate the antiferromagnetic solutions.

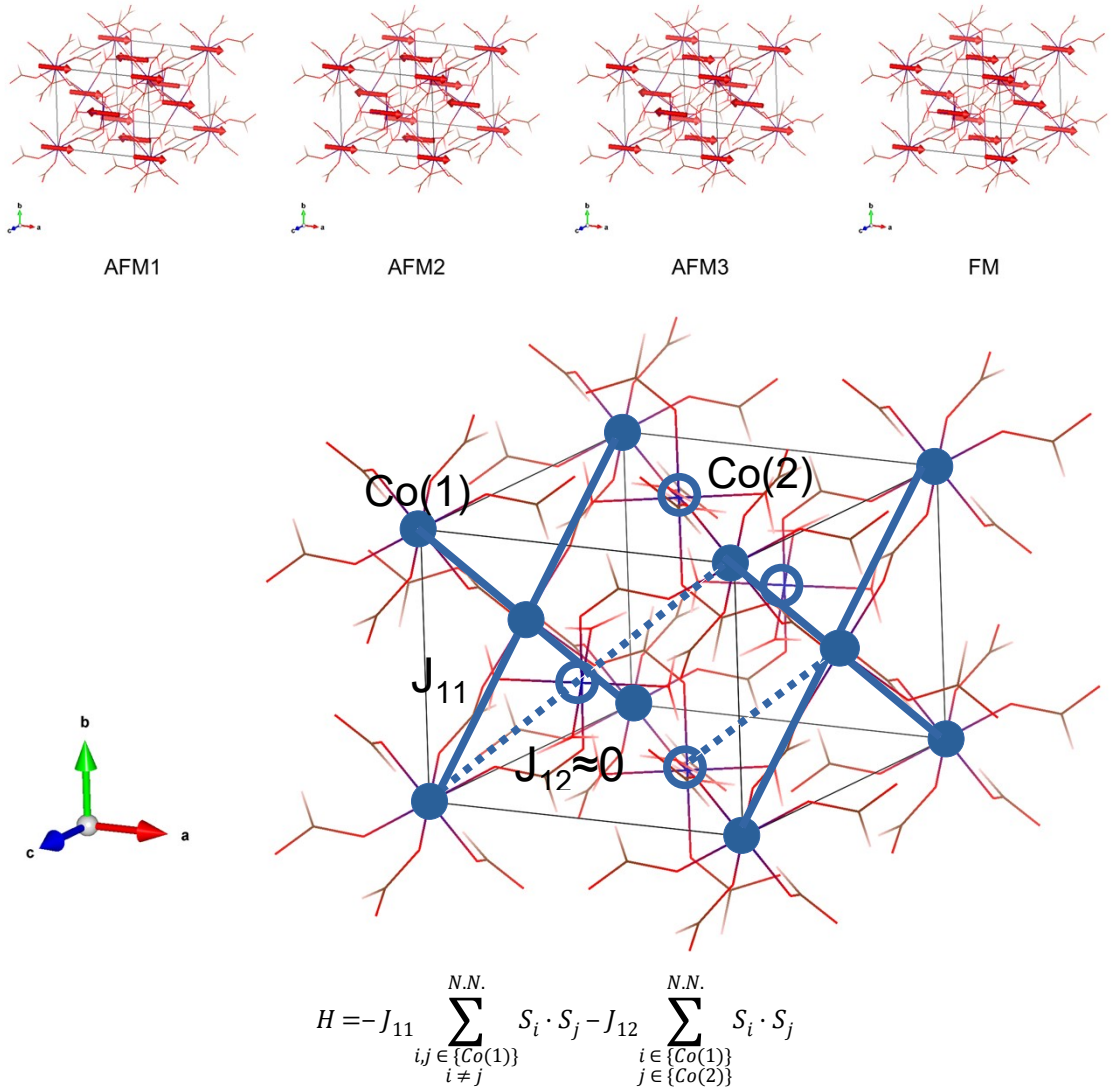

$$H = -J_{11} \sum_{\substack{i,j \in \{Co(1)\} \\ i \neq j}}^{N.N.} S_i \cdot S_j - J_{12} \sum_{\substack{i \in \{Co(1)\} \\ j \in \{Co(2)\}}}^{N.N.} S_i \cdot S_j$$

Figure SI1: Scheme of the magnetic orderings considered in the DFT calculations. Magnetic exchanges paths. According to the AFM1, AFM2 and AFM3 spin arrangements, the magnetic exchanges are derived as: $2J_{12} = ½(E(AFM2) - E(AFM3))$, whereas $4J_{11} = ½(E(AFM1) - E(AFM3))$. Indeed $J_{12} \approx 0.75\ meV$ and $J_{11} \approx 3\ meV$ at $U = 0$.

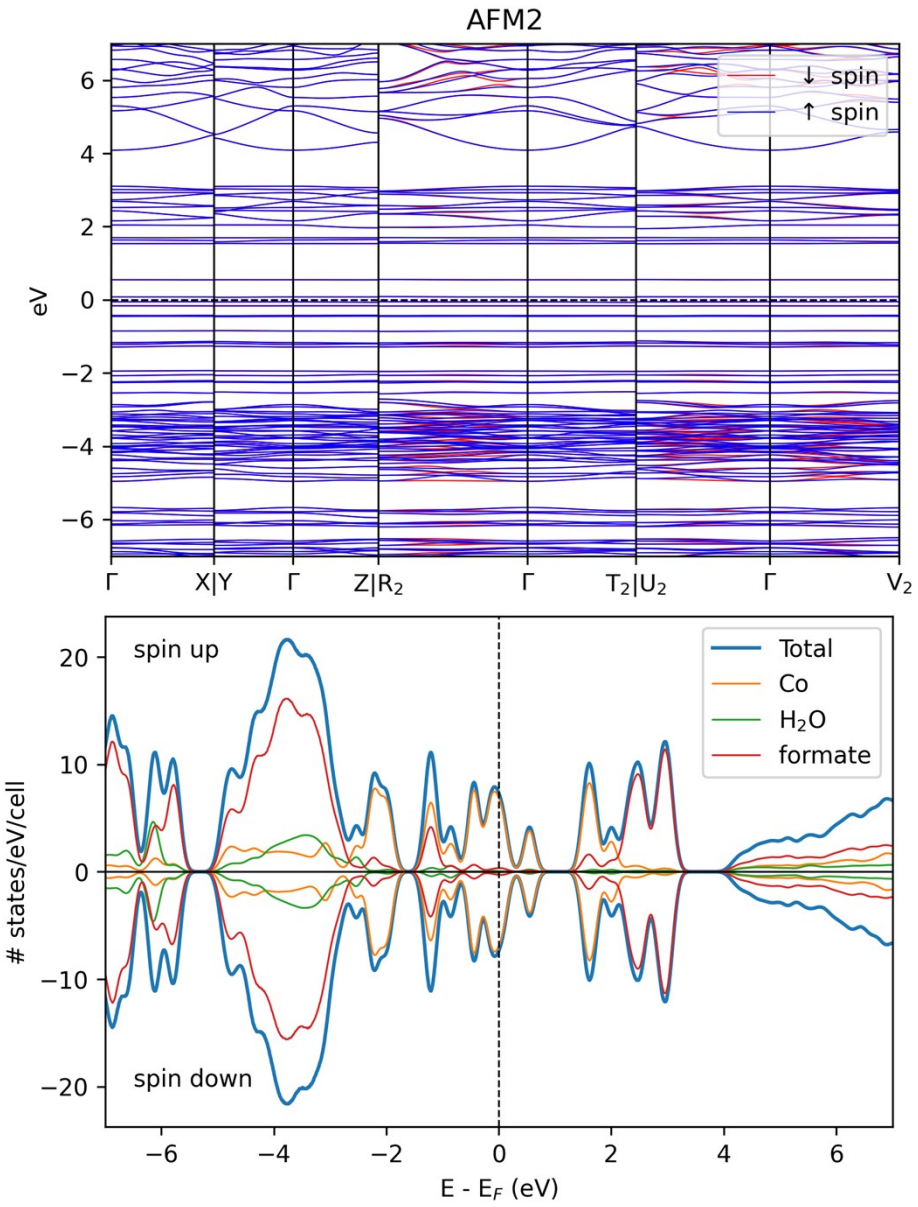

Figure SI2: Band structure and density of states of the AFM2 structure.

U (eV)	E(NM)-E(FM)	E(AFM1)-E(FM)	E(AFM2)-E(FM)	E(AFM3)-E(FM)
0	0.613	− 0.036	− 0.057	− 0.060
1	0.951	0.130	− 0.007	− 0.009
2	1.242	0.000	− 0.005	− 0.004
3	1.532	0.026	0.000	0.000
4	1.826	0.003	− 0.001	− 0.001

Table SI1: Total energy difference from the ferromagnetic (FM) solution, in eV/formula units, as a function of the Hubbard U value.

U	Co(1)-O(1)	Co(1)-O(3)	Co(1)-O(4)	Co(2)-O(2)	Co(2)-O(5)	Co(2)-O(6)
AFM1						
0	2.133 (0.71%)	2.069 (1.07%)	2.040 (1.28%)	2.175 (2.49%)	2.014 (− 0.32%)	2.122 (1.47%)
1	2.113 (0.59%)	2.073 (1.07%)	2.037 (1.25%)	2.175 (2.96%)	2.026 (0.28%)	2.153 (2.21%)
2	2.116 (0.87%)	2.091 (1.14%)	2.066 (1.47%)	2.191 (2.95%)	2.029 (0.42%)	2.140 (2.18%)
3	2.107 (0.78%)	2.092 (1.43%)	2.067 (1.76%)	2.188 (3.39%)	2.034 (0.65%)	2.139 (1.97%)
4	2.118 (1.43%)	2.091 (1.45%v	2.079 (2.31%)	2.200 (3.85%)	2.045 (1.21%)	2.145 (2.15%)
AFM2						
0	2.116 (0.71%)	2.086 (1.07%)	2.061 (1.28%)	2.171 (2.49%)	2.012 (− 0.45%)	2.125 (1.47%)
1	2.113 (0.59%)	2.087 (1.07%)	2.061 (1.25%)	2.181 (2.96%)	2.022 (0.06%)	2.141 (2.21%)
2	2.119 (0.87%)	2.088 (1.14%)	2.065 (1.47%)	2.181 (2.95%)	2.032 (0.54%)	2.140 (2.18%)
3	2.117 (0.78%)	2.094 (1.43%)	2.071 (1.76%)	2.190 (3.39%)	2.036 (0.73%)	2.136 (1.97%)
4	2.131 (1.43%)	2.094 (1.45%)	2.082 (2.31%)	2.200 (3.85%)	2.052 (1.53%)	2.140 (2.15%)
AFM3						
0	2.124 (1.09%)	2.091 (1.29%)	2.063 (1.37%)	2.169 (2.39%)	2.012 (− 0.44%)	2.127 (1.53%)
1	2.114 (0.61%)	2.086 (1.06%)	2.060 (1.24%)	2.181 (2.95%)	2.026 (0.24%)	2.138 (2.09%)
2	2.119 (0.88%)	2.088 (1.12%)	2.065 (1.47%)	2.181 (2.95%)	2.032 (0.56%)	2.140 (2.14%)
3	2.117 (0.78%)	2.094 (1.43%)	2.071 (1.76%)	2.190 (3.39%)	2.036 (0.74%)	2.136 (1.97%)
4	2.131 (1.44%)	2.094 (1.45%)	2.082 (2.31%)	2.200 (3.84%)	2.052 (1.54%)	2.140 (2.15%)
FM						
0	2.119 (0.88%)	2.086 (1.06%)	2.052 (0.82%)	2.161 (2.00%)	2.065 (2.20%)	2.096 (0.04%)
1	2.114 (0.62%)	2.096 (1.52%)	2.056 (1.01%)	2.184 (3.11%)	2.021 (0.03%)	2.140 (2.16%)
2	2.116 (0.72%)	2.091 (1.31%)	2.066 (1.53%)	2.191 (3.40%)	2.029 (0.40%)	2.141 (2.20%)
3	2.119 (0.85%)	2.095 (1.50%)	2.073 (1.84%)	2.198 (3.73%)	2.036 (0.76%)	2.142 (2.25%)
4	2.126 (1.19%)	2.097 (1.57%)	2.078 (2.08%)	2.200 (3.86%)	2.052 (1.53%)	2.137 (2.01%)
NM						
0	2.085 (− 0.76%)	2.028 (− 1.79%)	2.010 (− 1.25%	2.294 (8.27%)	1.946 (− 3.72%)	1.977 (− 5.60%)
1	2.128 (1.31%)	1.997 (− 3.27%)	1.986 (− 2.42%	2.326 (9.80%)	1.946 (− 3.69%)	1.980 (− 5.49%)
2	2.169 (3.24%)	1.988 (− 3.69%)	1.972 (− 3.13%)	2.333 (10.1%)	1.950 (− 3.49%)	1.987 (− 5.16%)
3	2.174 (3.47%)	1.991 (− 3.57%)	1.975 (− 2.94%)	2.320 (9.53%)	1.952 (− 3.42%)	1.994 (− 4.80%)
4	2.169 (3.27%v	1.999 (− 3.18%)	1.979 (− 2.78%)	2.318 (9.42%)	1.956 (− 3.20%)	2.002 (− 4.40%)
Expt.						
N/a	2.101	2.064	2.035	2.119	2.021	2.095

Table SI2: Co-O bond lengths in Å, as a function of U in eV. Values in parenthesis are the relative errors. Last section in bold are the experimental bond lengths from Table SI4.

U	**Co(1) pop**	**Co(1) magn**	**Co(2) pop**	**Co(2) magn**
AFM1				
0	7.450	2.510	7.471	2.477
1	7.447	2.514	7.446	2.511
2	7.398	2.571	7.400	2.562
3	7.374	2.597	7.380	2.585
4	7.338	2.636	7.348	2.621
AFM2				
0	7.451	2.509	7.465	2.480
1	7.429	2.535	7.431	2.523
2	7.399	2.569	7.404	2.555
3	7.370	2.601	7.378	2.587
4	7.337	2.637	7.350	2.618
AFM3				
0	7.436	2.526	7.499	2.437
1	7.428	2.537	7.431	2.523
2	7.399	2.570	7.404	2.556
3	7.370	2.602	7.378	2.587
4	7.337	2.637	7.350	2.618
FM				
0	7.421	2.542	7.466	2.483
1	7.429	2.536	7.431	2.526
2	7.398	2.570	7.400	2.562
3	7.368	2.604	7.373	2.593
4	7.337	2.638	7.345	2.624
NM				
0	7.781	0	7.778	0
1	7.783	0	7.778	0
2	7.774	0	7.775	0
3	7.762	0	7.766	0
4	7.748	0	7.752	0

Table SI3: Co population and magnetic moment (in μ_B) as a function of U in eV.

Cluster calculations on dimers of Co(1)-Co(1) and Co(1)-Co(2) were performed including all ligands for each site. Because of the charged nature of the system the formate ligands only coordinating to a single site in the cluster were capped with hydrogens to ensure charge neutrality in the calculation. Only the position of the hydrogen atoms were geometry optimised. The energies of each cluster were calculated enforcing either a ferromagnetic or an antiferromagnetic spin alignment between the two metal sites. The energies are shown in Table SI4 and SI5.

Both interactions are antiferromagnetic, decreasing as a function of U. However the Co(1)-Co(2) interaction in the dimer is stronger than in the Co(1)-Co(1) dimer, contrary to the experiment. This shows that calculations on finite clusters cannot be easily transferred to the solid. First, the Co(1)-Co(1) interactions are arranged in 2d planes, while the Co(1)-Co(2) interactions are along 1d chains. Second, the magnetic interactions in the crystal are not propagated by discrete energy level, but by continuous bands which can have different band-widths depending on the direction in k-space, hence on the direction in real space. Therefore, we can conclude that, the dimer approach confirms the AFM nature of the magnetic interactions at all values of U, although the cooperative interactions in the crystal show that the Co(1)-Co(2) exchange coupling is depressed.

$U\ (eV)$	$E_{FM}\ (Ry)$	$E_{AFM}\ (Ry)$	$E_{AFM} - E_{FM}\ \ (eV)$
0	-1457.8822043	-1457.8826689	-0.0063
1	-1457.8243280	-1457.8246419	-0.0043
2	-1457.7709089	-1457.7711343	-0.0031
3	-1457.7218875	-1457.7220667	-0.0024
4	-1457.6769147	-1457.6770350	-0.0016

Table SI4: Energies of a ferromagnetic and antiferromagnetic state in the Co(1)-Co(1) cluster with varying U.

$U\ (eV)$	$E_{FM}\ (Ry)$	$E_{AFM}\ (Ry)$	$E_{AFM} - E_{FM}\ \ (eV)$
0	-1282.9393963	-1282.9408841	-0.0202
1	-1282.8887240	-1282.8899576	-0.0168
2	-1282.8418539	-1282.8429537	-0.0150
3	-1282.7983296	-1282.7992976	-0.0132
4	-1282.7579375	-1282.7587880	-0.0116

Table SI5: Energies of a ferromagnetic and antiferromagnetic state in the Co(1)-Co(2) cluster with varying U.

2 MS MODEL

In the following section quality indicators of the model presented in the main script are included. These can be compared with similar quality indicators presented in the later two sections “High resolution MS model” and “GC model”, which are models briefly touched upon in the main script. At the end of the supporting information model parameters of all three models are included.

Besides quality indicators, geometry and parts of a topological analysis based on the framework of Bader[2] are included as well. The parts presented here are not necessary for the conclusions made in the main script, but are included for completeness.

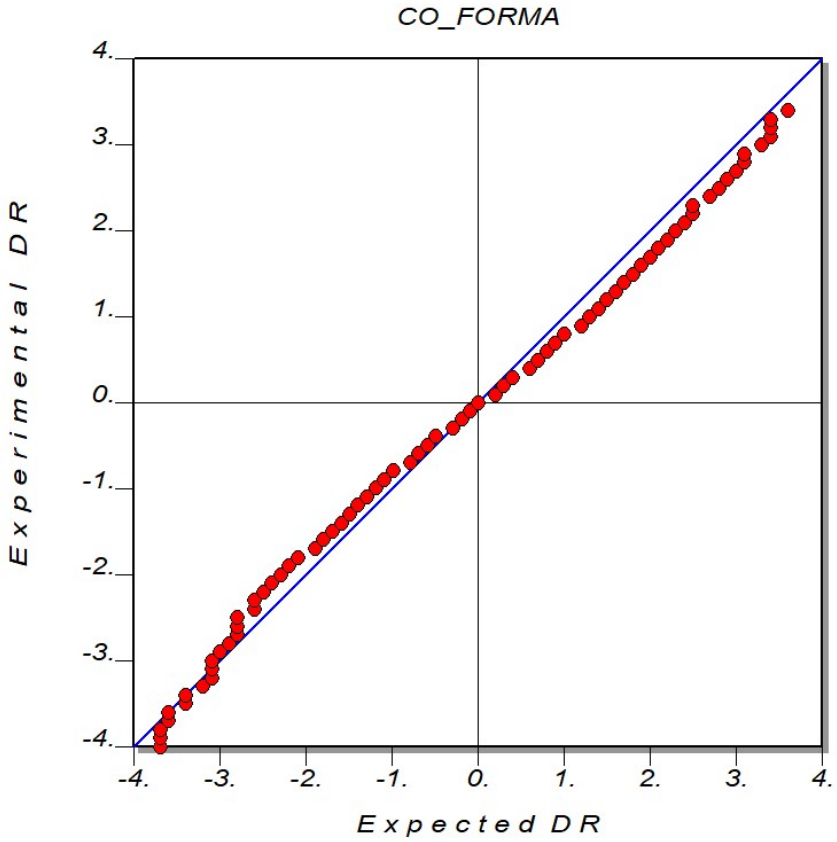

2.1 Normal probability plot

Figure SI3: Normal probability plot.

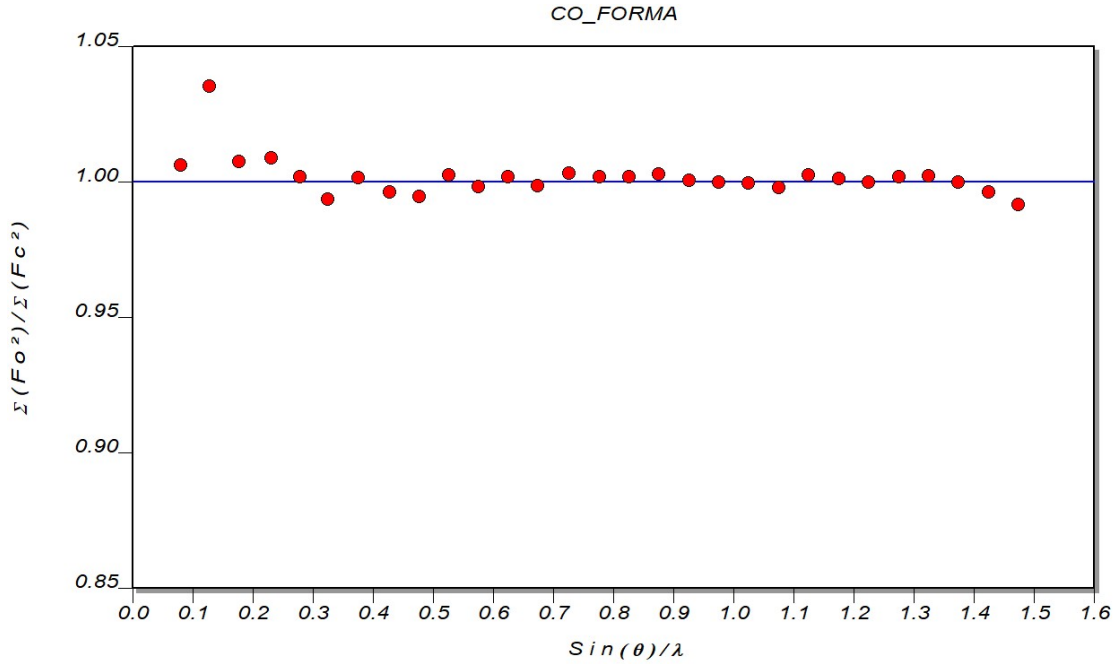

2.2 Scale plot

Figure SI4: Binned scale plot.

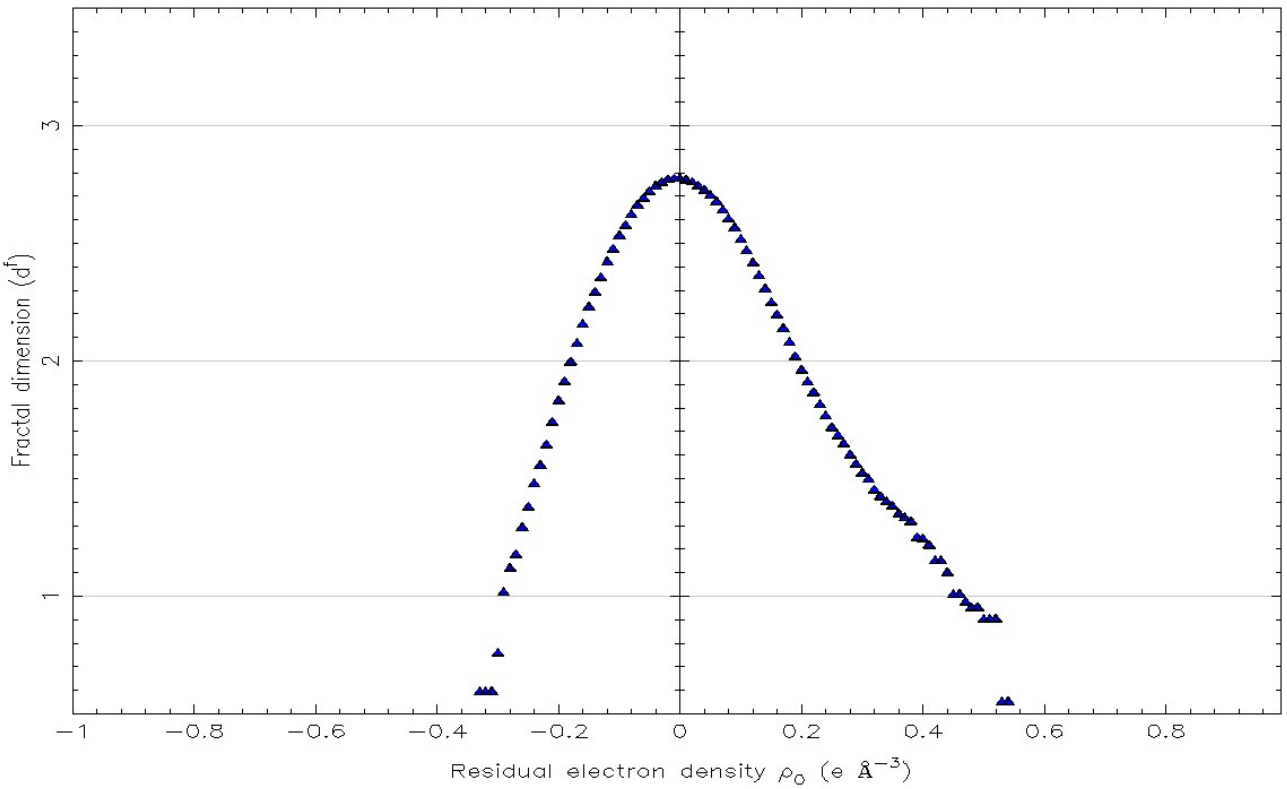

2.3 Fractal dimension plot 50x40x54 grid

Figure SI5: Fractal dimension plot. Evaluated grid is based on $\max n_x = 2\max h$, $\max n_y = 2\max k$, and $\max n_z = 2\max l$.

2.4 Geometry

The geometry derived from modelling the X-ray diffraction data is listed in Table SI6. Discrepancies between Co-O bond lengths in this model and the theoretical model is discussed in the main script. The experimental geometry includes refined H positions. This has been included to see to which extent modelling of the current data can yield reasonable X-H bond lengths. Ferraris & Franchini-Angela[3] studied a series of neutron scattering studies of crystalline hydrates. From the observed geometries they introduced a classification of water molecules based on their intra- and intermolecular geometries. This was further expanded by Chandler *et al*.[4] to include inorganic salts. H_2O in Co-formate belongs to the Class 1 group D (O(5), single coordinating planar) and Class 1' group J (O(6), single coordinating tetrahedral). The observed intervals of O-H bond length are $[0.858, 1.003]$ Å and $[0.917, 1.019]$ Å respectively as tabulated by Chandler *et al*. The refined O(5)-H bond length lies within the observed interval while O(6)-H are outside the interval unless two standard deviations are considered. This implies that the refined O(5)-H bond lengths are not unreasonable while the O(6)-H seem underestimated. However, it is also observed that trigonal planar water molecules tend to have shorter O-H bond lengths[5] whereas the O-H distances from the X-ray modelling shows O-H shorter for the tetrahedral water molecule. This further implies that the O-H distance of the tetrahedral molecule is underestimated from the experiment. This is not surprising given the shift of H valence into the bonding region, which typically underestimates the covalent X-H bond.

	Model $(25\ K)^b$
a [Å]	8.5472(3)
b [Å]	7.0177(2)
c [Å]	9.1727(3)
β [Å]	97.498(2)
O1-Co1-O4 [°]	92.513(6)
O1-Co1-O3 [°]	93.557(7)
O3-Co1-O4 [°]	90.332(6)
O2-Co2-O5 [°]	89.982(8)
O5-Co2-O6 [°]	90.586(7)
O2-Co2-O6 [°]	88.804(6)
Co1-O1 [Å]	2.10101(15)
Co1-O3 [Å]	2.06437(15)
Co1-O4 [Å]	2.03557(15)

Co2-O2 [Å]	2.11940(15)
Co2-O5 [Å]	2.02135(17)
Co2-O6 [Å]	2.09457(17)
C1-O1 [Å]	1.2471(2)
C1-O2 [Å]	1.2423(2)
C2-O3 [Å]	1.23897(19)
C2-O4 [Å]	1.2437(2)
C1-H1 [Å]	1.076(15)
C2-H2 [Å]	1.051(18)
O5-H(5A) [Å]	0.89(3)
O5-H(5B) [Å]	0.90(2)
O6-H(6A) [Å]	0.87(3)
O6-H(6B) [Å]	0.87(3)
O5-H5B···O2 [Å]	1.794(18)
O5-H5A···O3 [Å]	1.85(3)
O6-H6B···O1 [Å]	1.85(3)
O6-H6A···O4 [Å]	1.868(19)

Table SI6: Symmetry inequivalent angles of the Co octahedrons, geometric bond lengths of expected complex, covalent, & hydrogen bonds.

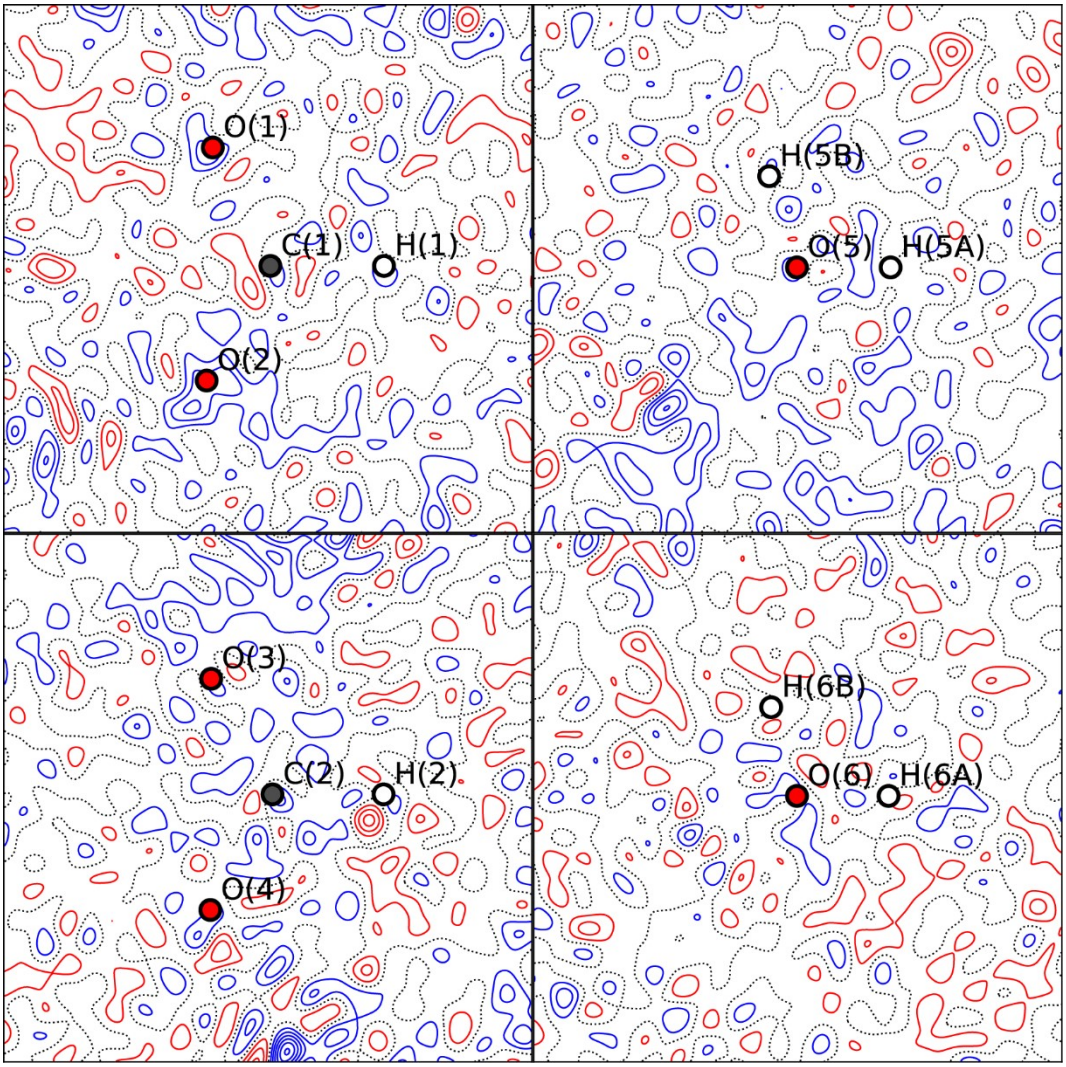

2.5 Residual Density

Figure SI6: Residual density maps through molecular planes. Contour levels in $0.10\ e/\text{Å}^{-3}$ intervals. Blue, red, and black represent positive values, negative values and the zero-contour.

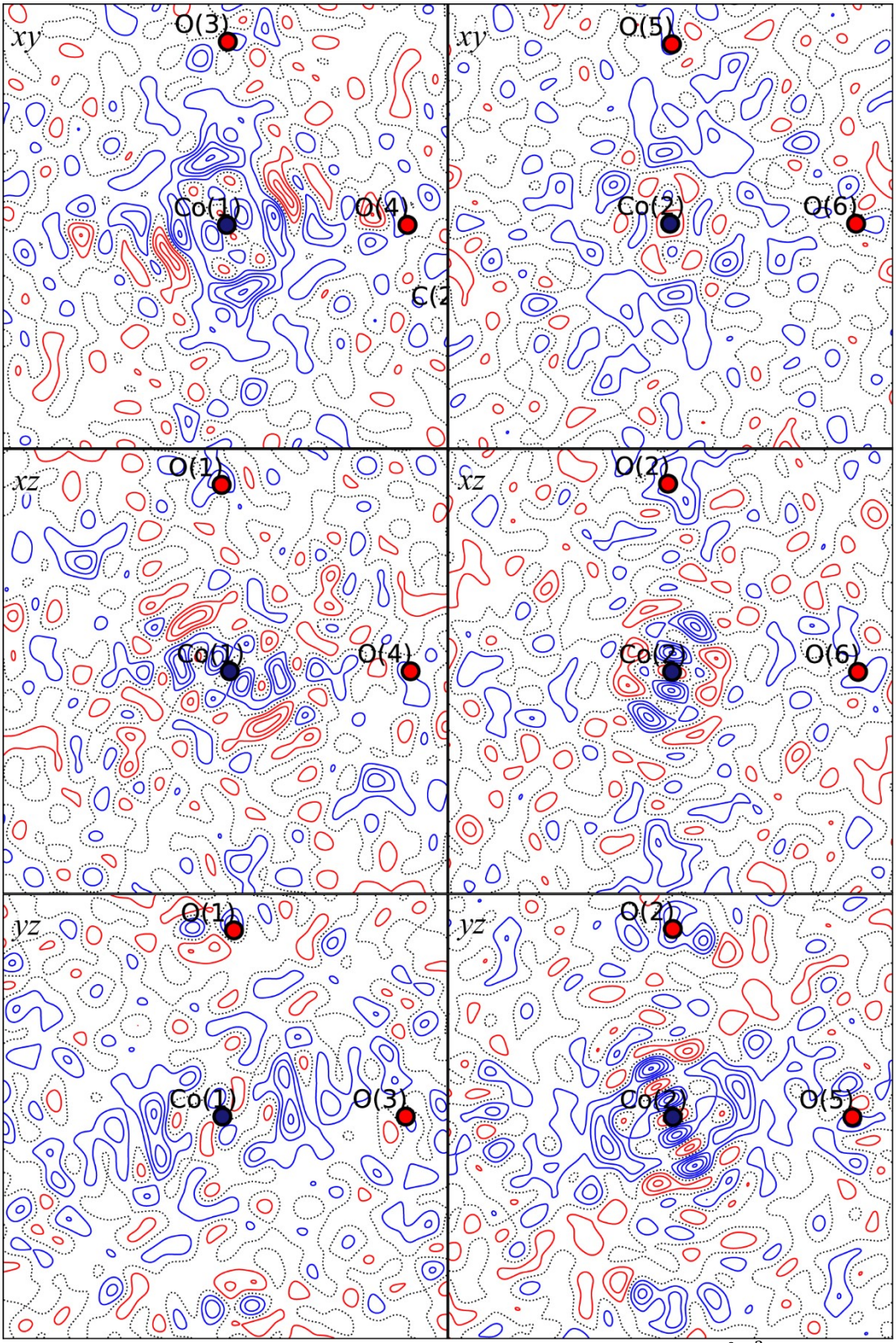

Figure SI7: Residual density maps through octahedron planes. Contour levels in $0.10\ e/\text{Å}^{-3}$ intervals. Blue, red, and black represent positive values, negative values and the zero-contour.

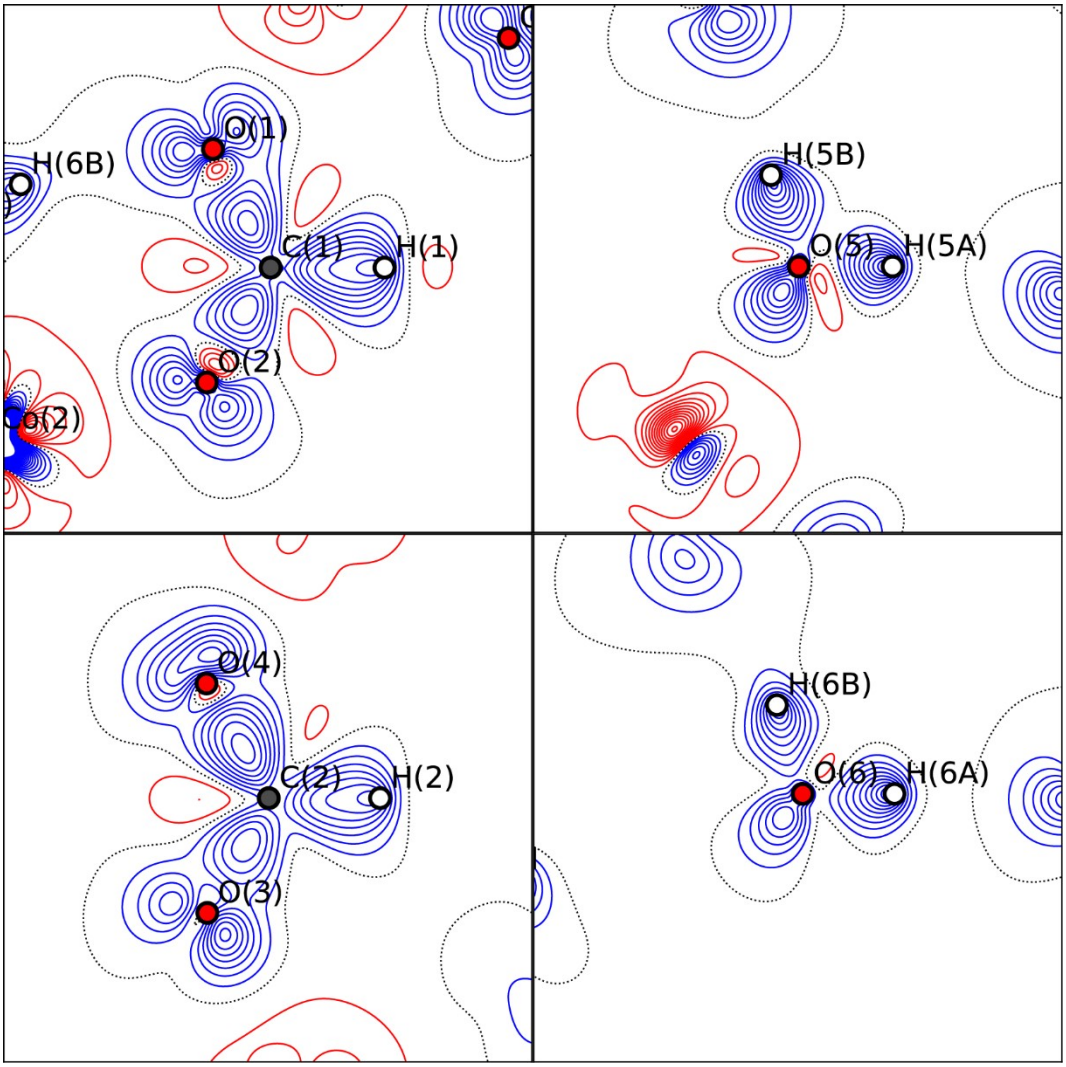

2.6 Deformation densities

Figure SI8: Deformation density maps (MM density subtracted IAM density) through molecular planes. Contour levels in $0.10\ e/\text{Å}^{-3}$ intervals. Blue, red, and black represent positive values, negative values and the zero-contour.

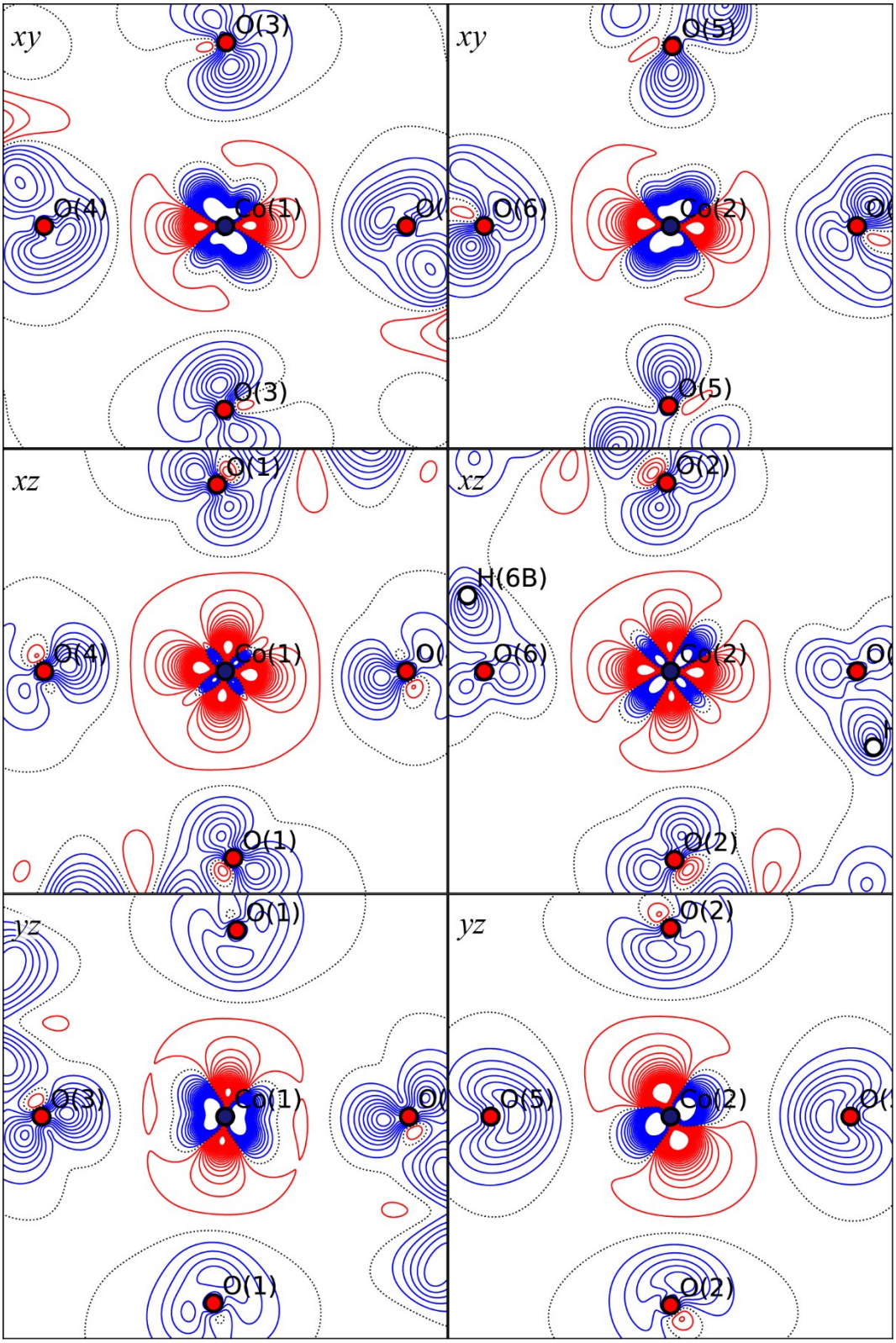

Figure SI9: Deformation density maps (MM density subtracted IAM density) through octahedron planes. Contour levels in $0.10\ e/\text{Å}^{-3}$ intervals. Blue, red, and black represent positive values, negative values and the zero-contour.

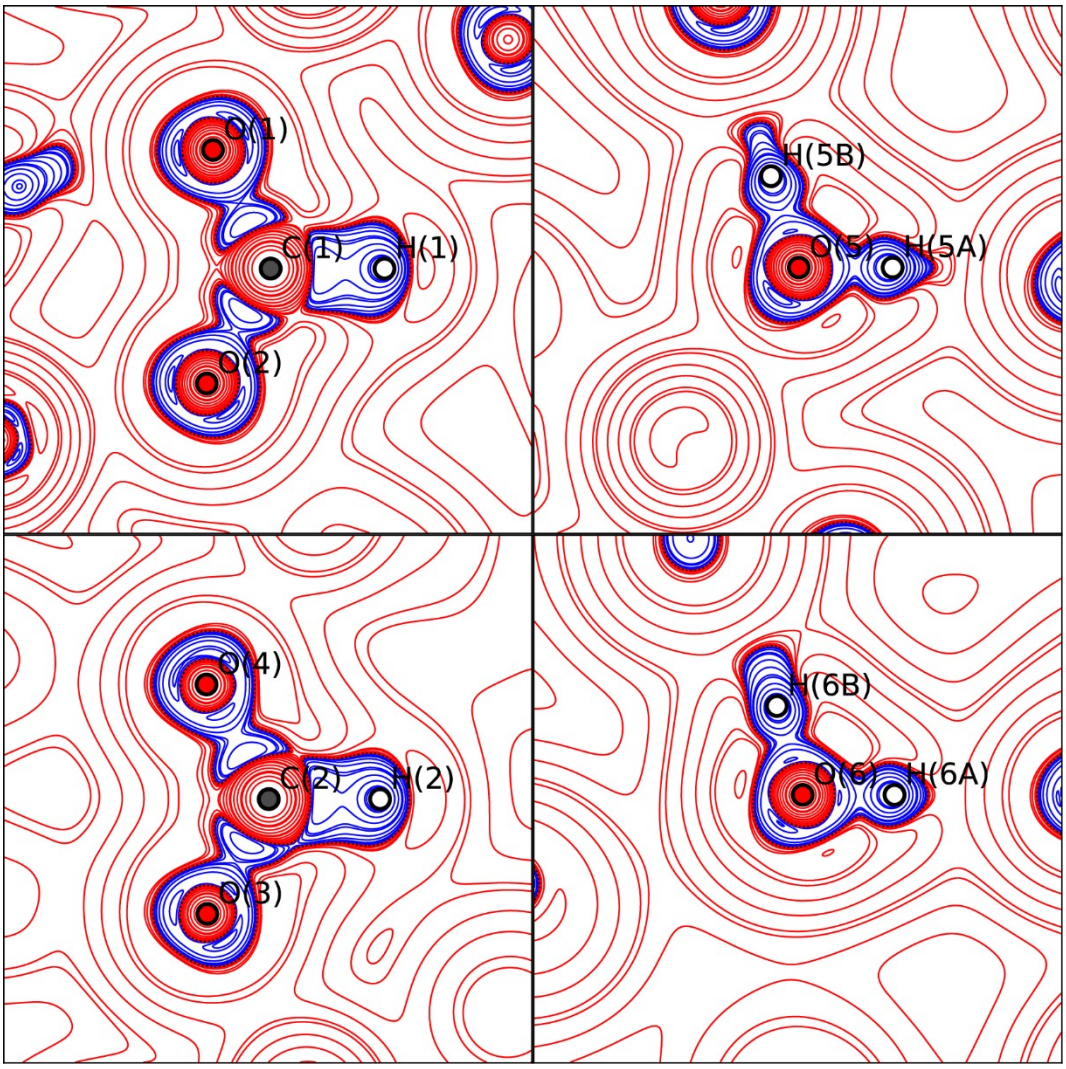

2.7 Laplacian

Figure SI10: Laplacian maps through molecular planes. The contour levels are at $\pm x \cdot 10^{y}\ e\ \text{Å}^{-5}$ with $x = 1, 2, 4, 8$ and $y = 0, \pm 1, \pm 2$. The blue and red lines represent charge concentration and depletion respectively.

2.8 Bond Critical Points

Table SI7 lists all symmetry inequivalent bond critical points (BCPs) located in the experimental density. These are consistent with expected bonds based on chemical intuition *i.e.* the intramolecular bonds of formate & water, the metal-ligand (M-L) interactions, and the hydrogen bonds are located. The nature of the interactions will be described based on the evaluated properties at the BCP in the following, see *e.g.* the review[6] given by Gatti for reference values.

The M-L interactions (first segment in Table SI7) overall have small densities and large positive Laplacians indicative, but not conclusively[7], of closed-shell interactions seen in dative interactions as expected for a coordination compound. This is further corroborated by the positive total energy density, H_b, and an excess of kinetic energy compared to potential energy. These features of the density all indicate that electron density is depleted at the BCP. Similar electron density and Laplacian values were obtained by Scatena *et al.*[8] for Cu-O interactions, which were characterised as dative with a varying amount of covalency. Similar to that study, the axial BCP relative to the chosen coordinate system shows a significantly smaller electron density at the BCP compared to the equatorial ligand BCPs indicating a weaker interaction. In contrast to the findings of Scatena *et al.* the ellipticity, ε, of the M-L interactions in Co-formate are large and similar to those observed for higher bond order carbohydrates chains[9]. Especially the linking formate between Co(1) and Co(2) shows a large ε, which can indicate the presence of higher order bonding. However, ε can as well be due to the aspherical electron density around the Co atom from the unequal d-orbital population. The energy densities on the other hand indicate that the bond between Co(1) and O(3) and the bond between Co(2) and O(5) are different form the remaining M-L bonds with larger potential energy compared to kinetic energy and smaller positive total energies indicating a larger degree of covalency in these bonds compared to the remaining M-L bonds.

The intramolecular BCPs of formate and water (second and third segment of Table SI7) all show large ρ_b, negative and large $\nabla^2\rho_b$, $|V_b|/G_b > 2$, and negative H_b/ρ_b consistent with open-shell interactions. A major difference between the BCPs in water compared to formate are the smaller ellipticities ε of the bonds. In water, ε is similar to values typical of single bonds (0.014 in butane) while ε for all bonds in formate have values

close to either one-and-a-half bond (0.176 in benzene) or double bond (0.298 in ethene) in hydrocarbon chains[9]. This indicates a delocalised double bond nature of the bonding interaction in formate, as is expected from chemical intuition.

The BCPs associated with hydrogen bonding (fourth segment in Table SI7) show small ρ_b, positive $\nabla^2\rho_b$, and $1 < |V_b|/G_b < 2$ consistent with hydrogen bonding, however, the $G_b/\rho_b < 1$ and negative H_b/ρ_b points towards a more open-shell interactions compared to typical hydrogen bonds. Because of the large uncertainty in $\nabla^2\rho$ related to the choice of the model, especially in connection with X-ray based densities and atomic positions of H, these features might be artefacts from the modelling. Furthermore, finer point of hydrogen bonds are better captured from evaluating the source function[10] and are only included here for completeness.

BCP	R_{ij}	d_{1-BCP}	d_{2-BCP}	ρ_b	$\nabla^2\rho$	ε	G_b	G_b/ρ_b	V_b	$\lvert V_b\rvert/G_b$	H_b/ρ_b
Co(1)-O(1)	2.1017	1.0205	1.0812	0.301	7.596	0.29	0.463	1.539	− 0.395	0.852	0.228
Co(1)-O(3)	2.0650	1.0199	1.0452	0.394	9.021	0.07	0.591	1.501	− 0.551	0.932	0.102
Co(1)-O(4)	2.0362	0.9867	1.0495	0.362	9.731	0.29	0.602	1.663	− 0.523	0.868	0.219
Co(2)-O(2)	2.1220	1.0285	1.0935	0.279	7.235	0.29	0.433	1.554	− 0.360	0.831	0.262
Co(2)-O(5)	2.0220	0.9973	1.0246	0.464	10.060	0.11	0.693	1.494	− 0.682	0.984	0.024
Co(2)-O(6)	2.0957	1.0084	1.0873	0.303	8.174	0.19	0.491	1.622	− 0.411	0.835	0.267
C(1)-H(1)	1.0759	0.7248	0.3510	1.952	− 23.086	0.13	1.373	0.704	− 4.364	3.176	− 1.532
C(1)-O(1)	1.2472	0.4522	0.7950	2.722	− 32.618	0.24	2.744	1.008	− 7.772	2.832	− 1.847
C(1)-O(2)	1.2426	0.4503	0.7923	2.668	− 30.255	0.28	2.714	1.017	− 7.547	2.780	− 1.811
C(2)-H(2)	1.0515	0.7153	0.3362	1.894	− 21.532	0.11	1.326	0.700	− 4.160	3.137	− 1.496
C(2)-O(3)	1.2391	0.4426	0.7965	2.690	− 28.212	0.17	2.867	1.066	− 7.708	2.689	− 1.800
C(2)-O(4)	1.2438	0.4355	0.8083	2.847	− 32.010	0.10	3.104	1.090	− 8.449	2.722	− 1.877
O(5)-H(5A)	0.8865	0.6834	0.2031	2.777	− 58.291	0.03	1.591	0.609	− 7.462	4.414	− 2.078
O(5)-H(5B)	0.9029	0.7028	0.2001	2.822	− 69.104	0.03	1.306	0.463	− 7.450	5.705	− 2.177
O(6)-H(6A)	0.8677	0.6816	0.1860	2.863	− 61.748	0.02	1.759	0.615	− 7.842	4.457	− 2.124
O(6)-H(6B)	0.8749	0.6916	0.1833	2.746	− 59.355	0.03	1.559	0.568	− 7.274	4.665	− 2.081
O(1)-H(6B)	1.8522	1.1361	0.7160	0.308	2.093	0.01	0.211	0.684	− 0.275	1.304	− 0.208
O(2)-H(5B)	1.7913	1.1422	0.6492	0.314	1.412	0.01	0.183	0.581	− 0.266	1.458	− 0.267
O(3)-H(5A)	1.8416	1.1597	0.6819	0.271	1.830	0.02	0.177	0.652	− 0.225	1.278	− 0.179
O(4)-H(6A)	1.8665	1.1713	0.6952	0.254	2.200	0.02	0.185	0.727	− 0.215	1.166	− 0.120

Table SI7: Observed symmetry inequivalent bond critical points in the structure. First segment relates to bonds in the coordination complexes, second segment to the two formate groups, third segment to the bonds within water, and fourth segment to hydrogen bonds between formate and water.
The columns correspond to the bond length, distance from atom 1 and 2 to the BCP, and density, Laplacian, ellipticity, kinetic energy density, kinetic energy per electorn, potential energy density, absolute ratio between potential and kinetic energy, & total energy per electron at the BCP. Distances are in Å, electron density in $e\,\text{Å}^{-3}$, laplacian in $e\,\text{Å}^{-5}$, energy densities in $Hartree\,\text{Å}^{-3}$, and energy per electron in $Hartree\,e^{-1}$. The uncertainties on especially the Laplacian is significantly underestimated from the least-squares procedure. This originates from the assumption of the model being the correct description. Minor changes in the electron density can translate into major changes in the Laplacian [11,12].
The kinetic energy density is calculated form the Abramov approximation[13] and with this values the potential energy density is calculated form the local virial theorem[2].

2.9 d-orbital populations in different coordinate systems

The d-orbital populations depend on the chosen coordinate system. In the main manuscript one of the chosen coordinate systems are used to argue for the orbital order and hence a ligand-field model. Here we present the populations when the coordinate system is oriented differently, however, still adhering to the local octahedral pseudo-symmetry. The populations written in the main manuscript are also included for comparison. The major effect of reorienting the coordinate system such that the z-axis points towards a new ligand is changing the populations of the e_g-orbitals and relabelling the individual t_{2g}-orbitals. Relative to the proposed ligand-field splitting the consequence is whether d_{z^2} or $d_{x^2-y^2}$ is the most stable e_g-orbital while the orbitals in the t_{2g}-set are relabelled.

Atom	Coordinate system (x,y,z)	d_{z^2}	$d_{x^2-y^2}$	d_{xy}	d_{xz}	d_{yz}	Total population
Co(1)	$(O(4), O(3), O(1))$	14.6	18.3	25.2	18.1	23.8	7.09
	$(O(1), O(3), O(4))$	14.4	18.2	24.0	18.5	25.0	
	$(O(4), O(1), O(3))$	20.7	12.4	18.3	25.1	23.5	
	Minimal cross terms	20.9	15.1	15.7	24.6	23.8	
Co(2)	$(O(6), O(5), O(2))$	14.1	18.0	24.4	22.7	20.8	7.12
	$(O(2), O(5), O(6))$	13.6	18.7	20.9	22.6	24.1	
	$(O(6), O(2), O(5))$	20.9	10.8	23.4	24.1	20.8	
	Minimal cross terms	22.2	17.0	16.1	20.4	24.4	

Table SI8: d-orbital populations of Co(1) and Co(2) in percentages of total population for ligand oriented coordinate systems. The minimal cross term system orientation is described in the main text.

The minimal cross terms systems follow the coordinate system choice of Sabino & Coppens.[14] For Co(1) the determined coordinate system corresponds to aligning z approximately towards O(3) and rotating the y-axis $\sim 30°$ anticlockwise about the z-axis away from O(1). For Co(2) the determined coordinate system correspond to aligning the z-axis approximately towards O(5) and rotating the y-axis $\sim 24°$ clolckwise about the z-axis away from O(6). Therefore, the minimal cross terms systems are approximately the ones with ligand oriented axes and the z-axis towards O(3) and O(5) for Co(1) and Co(2) respectively. These systems, however,

are more reminiscent of aligning the x- and y-axis in between the equatorial ligands (equatorial in the minimal cross terms coordinate system) moving away from the natural choice in an octahedron.

As there is no clear choice at low symmetry, except minimising cross terms which moves away from the natural choice in an octahedron, we decide to use the axis system described in the main script, *i.e.* the one with special axis towards the unique formate. Picking any of the other ligand oriented systems leads to the same conclusions. It would be possible to use any of the other ligand oriented coordinate systems, however, because the major argument in the main script follows from the relative t_{2g}-orbital energies, this would only lead to a relabelling of the orbitals.

2.10 Bader Charges

Bader charges have been evaluated for all atoms on a spherical grid $\varphi \times \theta \times r$ of $64 \times 48 \times 120$ points inside the atoms' β-sphere. The β-sphere is chosen such that the radius is just below the closest BCP. Outside the β-sphere, ray integration is performed using an angular grid of 64×48. The resulting charges and the integrated Lagrangian is listed in Table SI9. The Lagragian integrated within the atomic basis is analytically equal to 0^2 and can therefore be used to indicate whether the integration has converged. Ideally, it should be below 10^{-3}[15].

Co shows Bader charges close to its formal oxidation state of $+II$. Similarly, adding the charge of atoms within a molecular fragment gives -0.87 and -0.80 for formate 1 and formate 2 respectively and -0.02 and -0.13 for water 5 and water 6 respectively (naming water by constituent oxygen number). With charges close to the formal oxidation state the interactions seem overall in agreement with an interaction picture of water and formate coordinating lone-pairs towards the metal centre. This is especially true for the Co-OH_2 interaction where the Bader charge of water is almost 0. That the water is negatively charged, however, is an indication for them receiving electron density, but the underlying interaction for this is unclear at current point as water 6 does not have any orbitals oriented towards Co of proper symmetry allowing for back-donation.

	Q	L
Co1	1.81	$5.18 \cdot 10^{-4}$

Co2	1.78	$2.33 \cdot 10^{-4}$
O1	− 1.20	$4.16 \cdot 10^{-4}$
O2	− 1.11	$5.80 \cdot 10^{-4}$
O3	− 1.16	$4.26 \cdot 10^{-4}$
O4	− 1.27	$4.61 \cdot 10^{-4}$
O5	− 1.10	$4.75 \cdot 10^{-4}$
O6	− 1.08	$4.85 \cdot 10^{-4}$
C1	1.39	$-1.05 \cdot 10^{-5}$
C2	1.56	$1.89 \cdot 10^{-3}$
H1	0.05	$2.35 \cdot 10^{-4}$
H2	0.07	$1.90 \cdot 10^{-4}$
H5A	0.52	$4.31 \cdot 10^{-4}$
H5B	0.57	$1.13 \cdot 10^{-3}$
H6A	0.50	$3.13 \cdot 10^{-4}$
H6B	0.48	$6.60 \cdot 10^{-4}$
Formate 1	− 0.87	N/a
Formate 2	− 0.80	N/a
Water 5	− 0.01	N/a
Water 6	− 0.10	N/a
Total	0.02	N/a

Table SI9: Integrated properties within the atomic basin defined in QTAIM as the atom. Q is the atomic Bader charge defined as the neutral atomic electron population subtracted the electronic population within the atomic basin. L is the integrated Lagrangian.
The charges of formate 1, formate 2, water 5, and water 6 are the summed charges of the constituent atoms forming the molecules, where the formate are named as previously and water 5 is composed of O(5) and water 6 is composed of O(6). Total is the sum of all charges accounting for site symmetry and is a measure of the convergence of the integration. N/a is shorthand for not applicable.

3 HIGH RESOLUTION MS MODEL

Peaks are observed out to at least $\sin\theta/\lambda = 1.7$ Å^{-1}, however, the final model only includes reflections out to 1.5 Å^{-1}. The model presented in the main script has been tested against a larger resolution following the same refinement procedure and including the same parameters. The model converged within the same convergence criteria at the final iteration both before and after inclusion of SHADE H ADPs. However, κ did not converge for every step throughout the refinement strategy both before and after the inclusion of H ADPs. In the following the scale, normal probability, and fractal dimension plot of the final converged model are included.

Normal probability does not shown any discrepancy and is similar to the one obtained from the reduced resolution. The scale plot, however, shows a systematic clear downward trend above $\sin\theta/\lambda = 1.5$ Å^{-1} and the fractal dimension plot shows a negative residual density shoulder and goes to larger positive residual density. From fractal dimension plots it is not possible to distinguish systematic errors in modelling from systematic errors in data measuring and reduction, however, given the consistent agreement between model and observations for peaks observed at $\sin\theta/\lambda < 1.5$ Å^{-1} it appears that the high resolution reflections are systematically mistreated or erroneously measured why we decided to exclude them from the refined model in the main script.

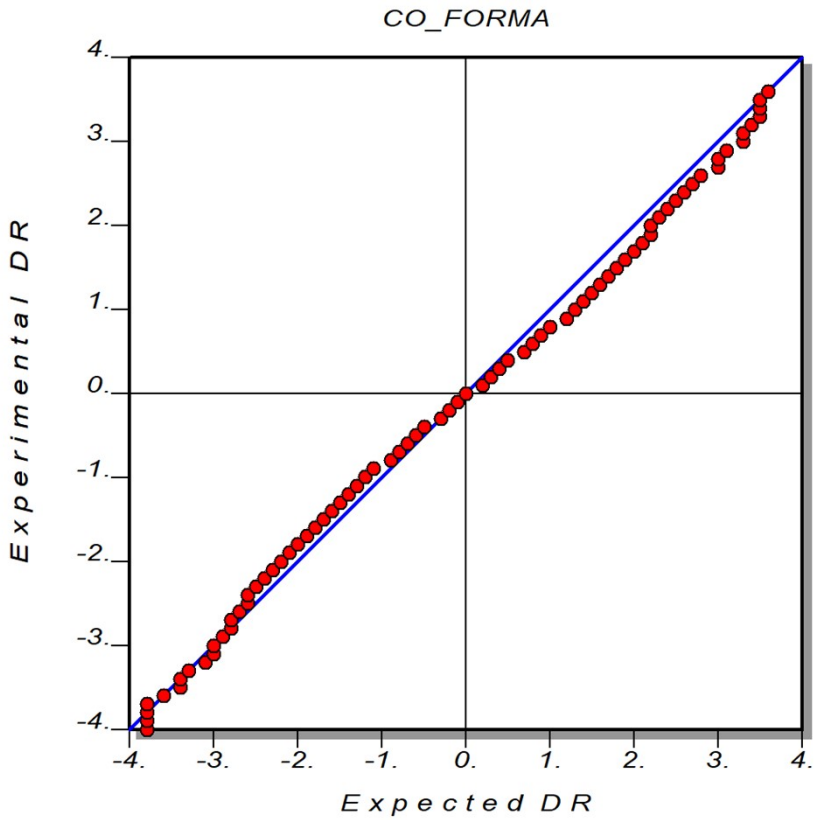

3.1 Normal probability plot

Figure SI11: Normal probability plot.

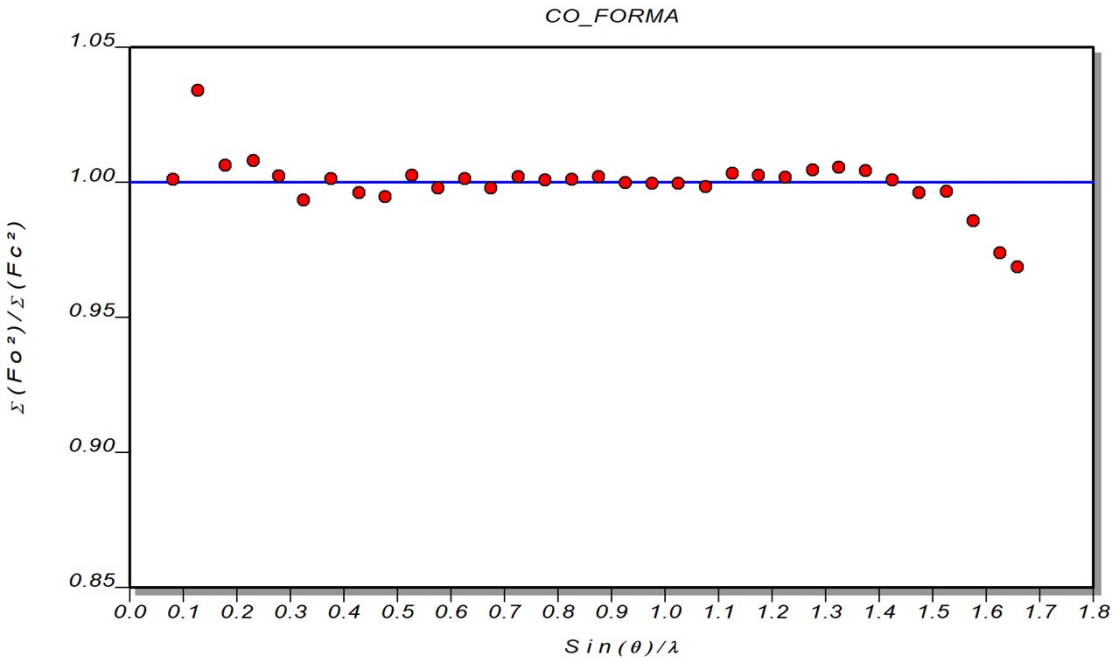

3.2 Scale plot

Figure SI12: Binned scale plot.

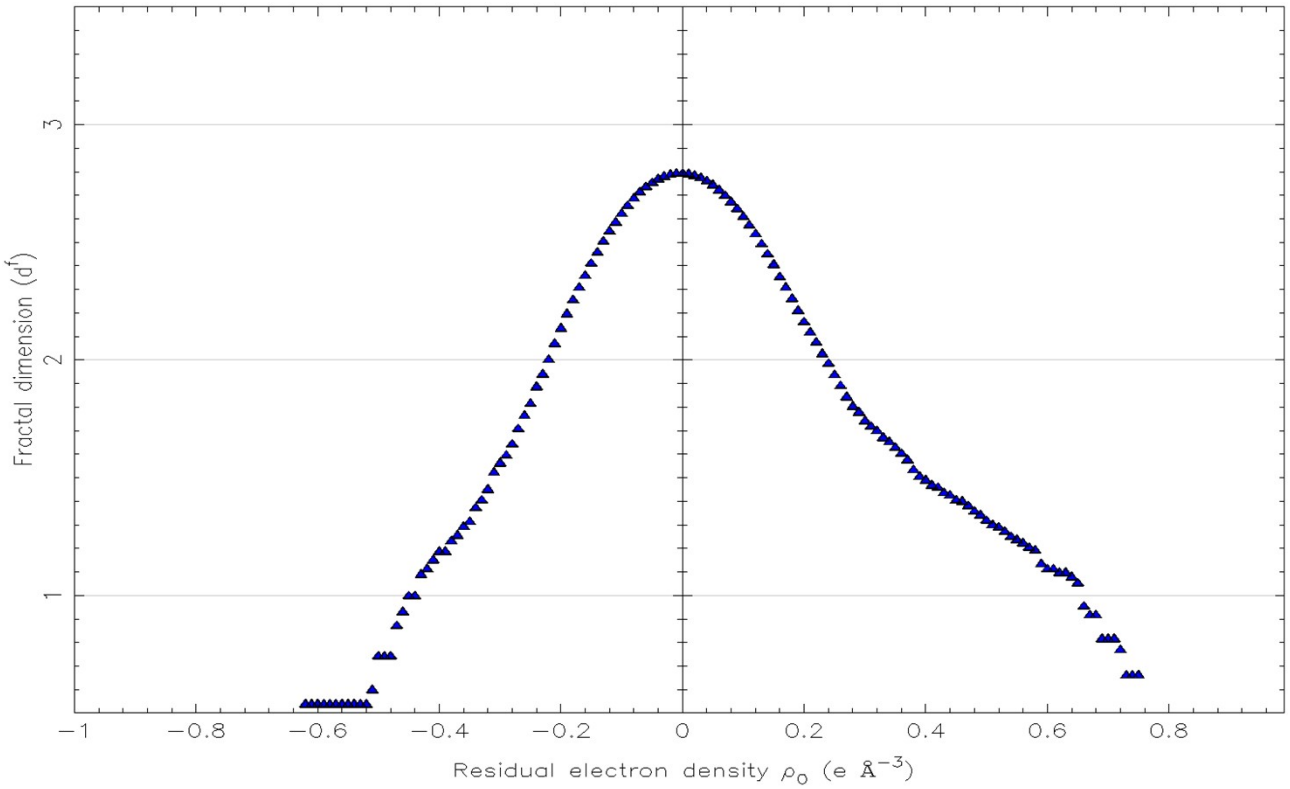

3.3 Fractal dimension plot 56x42x60 grid

Figure SI13: Fractal dimension plot. Evaluated grid is based on $\max n_x = 2\max h$, $\max n_y = 2\max k$, and $\max n_z = 2\max l$.

4 GC MODEL

The model has been refined equivalently to the model presented in the main script with the distinction of Gram-Charlier (GC) parameters being included for both Co atoms simultaneously with refining the remaining thermal parameters. Due to inversion symmetry 3rd order GC (γ^{ijk}) parameters are symmetry restricted to 0, while all 4th order GC (δ^{ijkl}) parameters are freely refinable. Only δ^{1111} and δ^{2222} are definitely significant within 3σ while the remaining δ^{ijkl} are either smaller than 3σ or 1 unit above 3σ on the first significant digit on both atoms. The inclusion of Gram-Charlier is inspired by the residual density in SI 1.5 on both Co atoms. These exhibit alternating positive and negative residuals, which is typically observed for anharmonically vibrating atoms[16].

The inclusion of Gram-Charlier reduces the shoulder at positive residuals observed in the fractal dimension plot, however, a shoulder is now apparent at negative residuals. Simultaneously, negative probability is observed for both atomic positions with the inclusion on the size of a few percentages.

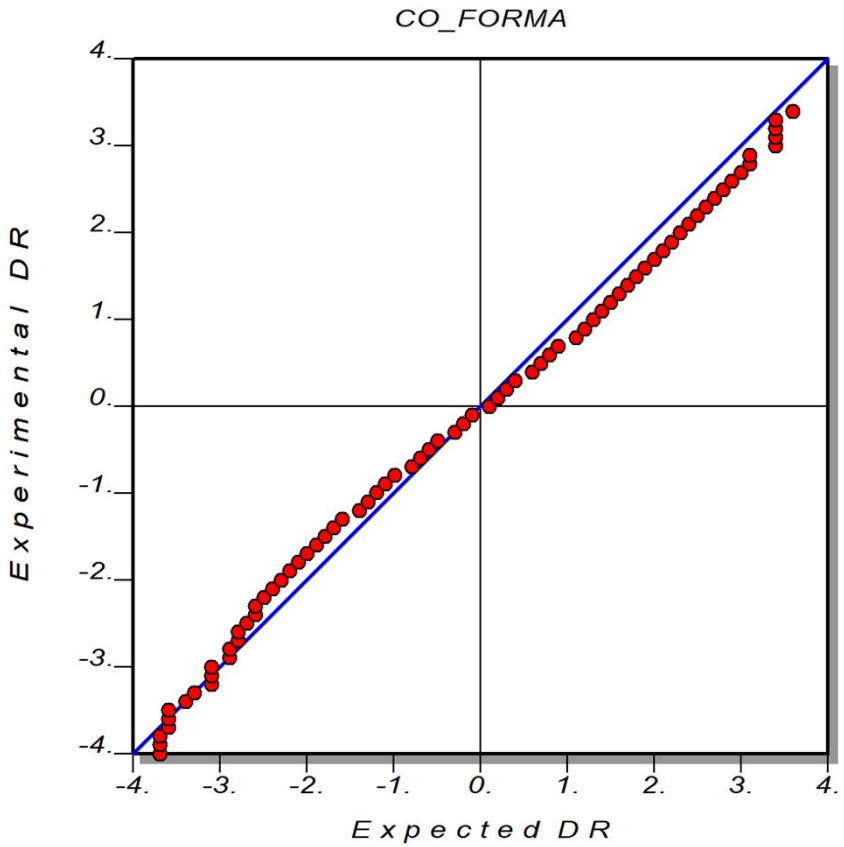

4.1 Normal probability plot

Figure SI14: Normal probability plot.

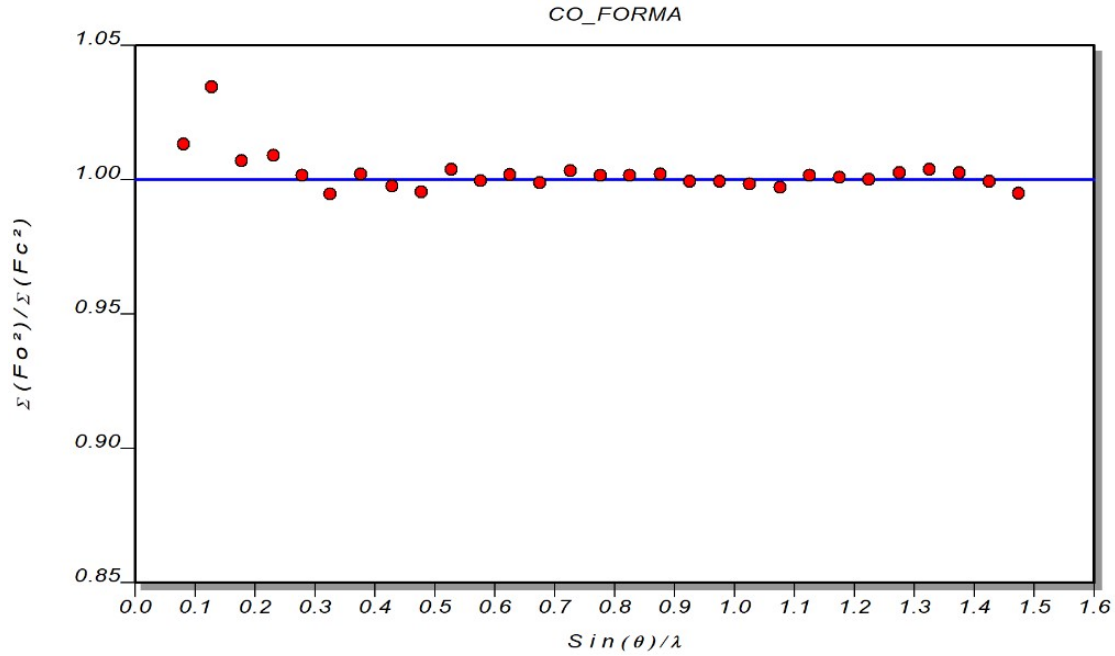

4.2 Scale plot

Figure SI15: Binned scale plot.

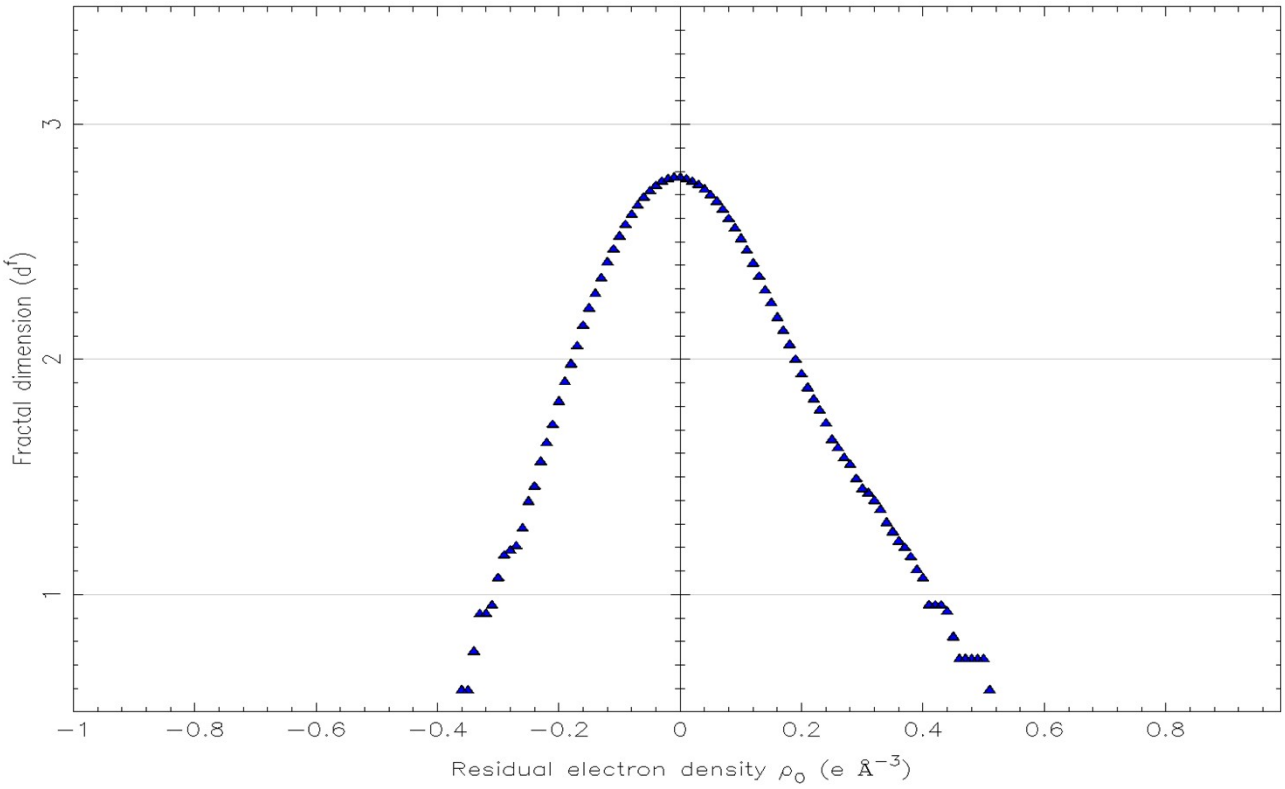

4.3 Fractal dimension plot 50x40x54 grid

Figure SI16: Fractal dimension plot. Evaluated grid is based on $\max n_x = 2\max h$, $\max n_y = 2\max k$, and $\max n_z = 2\max l$.

4.4 Nuclear Probability Density Functions

	Grid size	Grid dimension	Total negative probability	Total probability
Co(1)	$51 \times 51 \times 51$	$0.8 \times 0.8 \times 0.8$	− 3.320%	103.320%
Co(2)	$51 \times 51 \times 51$	$0.8 \times 0.8 \times 0.8$	− 1.776%	101.776%

Table SI10: The total negative probability and total probability of the anharmonically vibrating Co atoms. The probability is evaluated on a $51 \times 51 \times 51$ point grid spanning 0.8 Å in the 3 directions.

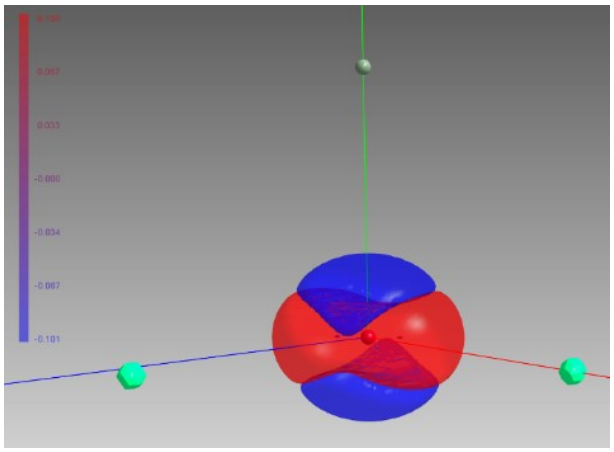

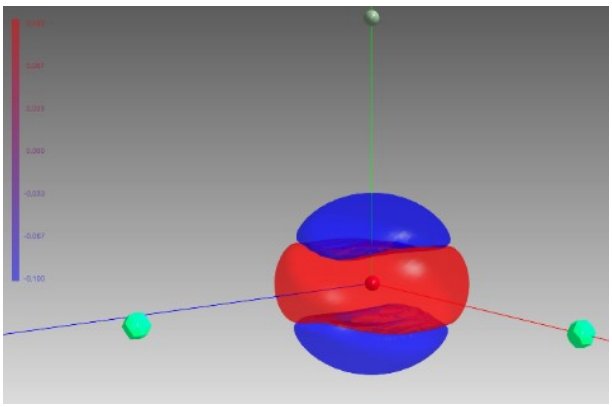

Figure SI17: Nuclear probability density function (nPDF) isosurface of Co(1) and Co(2), to the left and right respectively. Isosurface level at $\pm 0.1\ \text{Å}^{-3}$. Axes markers are $1\ \text{Å}$ away from the atomic sites. Blue represents negative nPDF, and red represents positive nPDF. Notice small inclusion of negative nPDF in the positive nPDF of Co(1) near the atomic site.

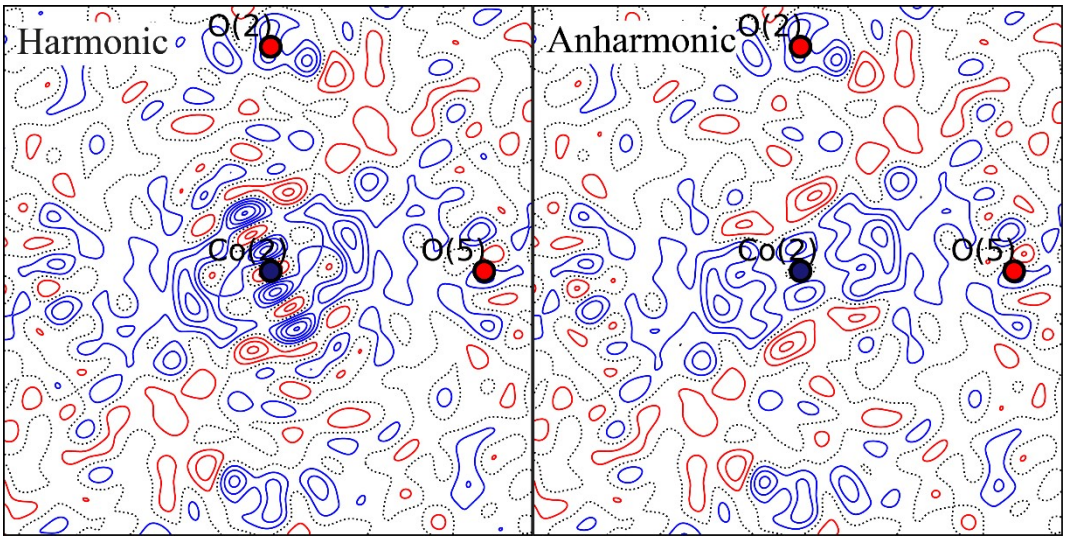

4.5 Residual Density

Figure SI18: Residual density map through the yz plane of Co(2) before and after 4th order Gram-Charlier refinement. The alternating residuals towards O(2) disappear but the GC parameters are not affecting the residuals towards O(5). Contour levels in $0.10\ e/\text{Å}^{-3}$ intervals. Blue, red, and black represent positive values, negative values and the zero-contour

4.6 d-orbital population

Atom	d_{z^2}	$d_{x^2-y^2}$	d_{xy}	d_{xz}	d_{yz}	Total population
Co(1)	13.6	18.7	25.8	18.8	23.1	7.14
Co(2)	16.2	15.2	22.8	23.4	22.4	7.19

Table SI11: d-orbital populations extracted by the method of Holladay *et al.* [17]. Notice that the population order of the Co(1) d-orbitals is unchanged while the population order of Co(2) changes in the e_g-set. Furthermore, the Co(1) d_{xy} and d_{yz} orbitals become more equivalently occupied with a small difference, albeit d_{yz} is still the least occupied t_{2g}-orbital.

5 MS MODEL PARAMETERS

5.1 Fractional coordinates

	x	y	z
Co(1)	0	0	0
Co(2)	0.5	0.5	0
O(1)	0.209584(16)	0.15649(2)	0.000174(16)
O(2)	0.437169(17)	0.22255(2)	− 0.078065(17)
O(3)	0.096917(16)	− 0.10148(2)	0.203110(15)
O(4)	0.089479(16)	− 0.228990(19)	− 0.097384(15)
O(5)	0.411021(18)	0.61025(3)	− 0.197070(17)
O(6)	0.721051(17)	0.47746(2)	− 0.073825(17)
C(1)	0.324965(18)	0.11460(2)	− 0.063870(18)
C(2)	0.033757(18)	− 0.27976(2)	− 0.223426(17)
H(1)	0.3244(12)	− 0.027(2)	− 0.1094(12)
H(2)	− 0.0720(19)	− 0.2164(15)	− 0.2715(12)
H(5A)	0.311(3)	0.5975(12)	− 0.2343(13)
H(5B)	0.4635(17)	0.6480(14)	− 0.271(2)
H(6A)	0.784(2)	0.398(3)	− 0.0234(19)
H(6B)	0.7614(17)	0.591(4)	− 0.0545(12)

Table SI12: Refined atomic coordinates given in fractions of the unit cell vectors.

5.2 Thermal Parameters

	U^{11} [Å^2]	U^{22} [Å^2]	U^{33} [Å^2]	U^{12} [Å^2]	U^{13} [Å^2]	U^{23} [Å^2]
Co(1)	0.003044(11)	0.003070(12)	0.002897(11)	0.000001(6)	0.000320(7)	− 0.000015(6)
Co(2)	0.003076(11)	0.003797(12)	0.003743(11)	− 0.000127(7)	0.000455(7)	0.000114(7)
O(1)	0.00496(3)	0.00625(4)	0.00772(4)	− 0.00098(3)	0.00202(3)	− 0.00057(3)
O(2)	0.00567(3)	0.00636(4)	0.00936(4)	− 0.00161(3)	0.00293(3)	− 0.00178(3)
O(3)	0.00609(3)	0.00654(4)	0.00529(3)	− 0.00075(3)	0.00025(3)	0.00183(3)
O(4)	0.00644(3)	0.00613(4)	0.00513(3)	0.00125(3)	− 0.00008(3)	− 0.00167(2)

O(5)	0.00573(4)	0.01346(5)	0.00667(4)	0.00001(3)	0.00041(3)	0.00344(3)
O(6)	0.00554(3)	0.00642(4)	0.00815(4)	0.00030(3)	0.00122(3)	0.00000(3)
C(1)	0.00509(4)	0.00534(4)	0.00830(4)	− 0.00089(3)	0.00205(3)	− 0.00119(3)
C(2)	0.00607(4)	0.00609(4)	0.00585(4)	0.00138(3)	− 0.00070(3)	− 0.00194(3)
H(1)	0.021547	0.013298	0.027729	− 0.002205	0.007962	− 0.009635
H(2)	0.014062	0.018194	0.016854	0.002536	− 0.001858	0.00103
H(5A)	0.010991	0.026493	0.019614	− 0.00539	− 0.003096	0.002171
H(5B)	0.018875	0.029169	0.014429	− 0.007011	0.004871	0.004583
H(6A)	0.016562	0.01552	0.025453	0.004093	0.000536	0.003248
H(6B)	0.017784	0.01259	0.02324	− 0.003437	0.001349	0.000035

Table SI13: Refined ADPs of the atoms. No uncertainty on H ADPs as these are locked to the ones derived from SHADE3.

5.3 Monopole Population & Shielding Constants

	P_0 [#e]	κ	κ'
Co(1)	3.547(17)	1.051(4)	1
Co(2)	3.559(17)	1.055(4)	1
O(1)	6.37(2)	0.9891(13)	0.99(2)
O(2)	6.30(2)	0.9891(13)	0.99(2)
O(3)	6.33(2)	0.9891(13)	0.99(2)
O(4)	6.38(2)	0.9891(13)	0.99(2)
O(5)	6.22(4)	0.996(2)	0.87(2)
O(6)	6.27(4)	0.996(2)	0.87(2)
C(1)	4.13(5)	0.996(5)	0.909(14)
C(2)	4.06(5)	0.996(5)	0.909(14)
H(1)	1.02(3)	1.1	1.18
H(2)	1.00(3)	1.1	1.18
H(5A)	0.97(3)	1.18	1.5
H(5B)	0.95(3)	1.18	1.5
H(6A)	0.96(3)	1.18	1.5
H(6B)	0.95(3)	1.18	1.5

Table SI14: Refined monopole populations and shielding constants (κ and κ'). For H the shielding constants are locked to the midpoint of observed values. These values depend on what atom H is bonded to and they are based on modelling theoretical densities[18].

5.4 Dipole Populations

	$P_{11}\,[\#e]$	$P_{1-1}\,[\#e]$	$P_{10}\,[\#e]$
Co(1)	0	0	0
Co(2)	0	0	0
O(1)	0.014(6)	0.001(6)	− 0.071(7)
O(2)	0.004(6)	− 0.001(6)	− 0.109(8)
O(3)	0.066(7)	− 0.002(7)	0.042(7)
O(4)	0.018(6)	0.015(6)	− 0.087(7)
O(5)	0.002(9)	− 0.026(12)	0.118(11)
O(6)	0.086(11)	− 0.077(12)	0.037(9)
C(1)	− 0.008(12)	− 0.011(13)	− 0.054(15)
C(2)	− 0.007(12)	0.010(13)	− 0.011(16)
H(1)	0	0	0.19(2)
H(2)	0	0	0.14(3)
H(5A)	0	0	0.12(3)
H(5B)	0	0	0.13(2)
H(6A)	0	0	0.10(3)
H(6B)	0	0	0.07(3)

Table SI15: Refined dipole populations. If a parameter was not refined it is given a population of 0.

5.5 Quadrupole Populations

	$P_{20}\,[\#e]$	$P_{21}\,[\#e]$	$P_{2-1}\,[\#e]$	$P_{22}\,[\#e]$	$P_{2-2}\,[\#e]$
Co(1)	− 0.077(5)	0.003(5)	0.036(5)	− 0.114(5)	0.098(5)
Co(2)	− 0.065(5)	0.011(4)	0.089(5)	− 0.067(5)	− 0.052(5)
O(1)	− 0.063(7)	− 0.030(6)	0.020(6)	− 0.025(6)	− 0.037(6)
O(2)	− 0.048(7)	− 0.008(6)	0.002(6)	− 0.029(6)	0.037(6)
O(3)	0.060(6)	− 0.034(6)	0.059(6)	− 0.038(6)	− 0.037(6)
O(4)	0.022(6)	− 0.039(6)	0.001(6)	− 0.056(6)	0.010(6)
O(5)	0.027(8)	0.002(8)	0.018(9)	0.123(10)	− 0.045(8)
O(6)	0.007(8)	− 0.051(8)	0.088(8)	− 0.000(8)	− 0.082(9)

C(1)	0.095(12)	0.064(11)	0.010(11)	− 0.231(14)	− 0.001(10)
C(2)	0.085(13)	− 0.032(10)	− 0.042(11)	− 0.323(16)	0.032(11)
H(1)	0	0	0	0	0
H(2)	0	0	0	0	0
H(5A)	0.082(16)	0	0	0	0
H(5B)	0.112(18)	0	0	0	0
H(6A)	0.056(18)	0	0	0	0
H(6B)	0.091(17)	0	0	0	0

Table SI16: Refined quadrupole populations. If a parameter was not refined it is given a population of 0.

5.6 Octupole Populations

	$P_{30}\,[\#e]$	$P_{31}\,[\#e]$	$P_{3-1}\,[\#e]$	$P_{32}\,[\#e]$	$P_{3-2}\,[\#e]$	$P_{33}\,[\#e]$	$P_{3-3}\,[\#e]$
Co(1)	0	0	0	0	0	0	0
Co(2)	0	0	0	0	0	0	0
O(1)	0.031(7)	− 0.000(6)	0.011(6)	0.013(6)	0.004(6)	− 0.007(6)	− 0.016(6)
O(2)	0.036(7)	0.005(6)	0.004(6)	0.009(6)	0.005(6)	− 0.002(6)	− 0.006(6)
O(3)	0.053(7)	− 0.009(6)	− 0.020(6)	0.005(6)	0.037(6)	− 0.015(6)	− 0.005(6)
O(4)	0.061(7)	0.012(6)	0.004(6)	0.021(6)	− 0.015(6)	0.011(6)	0.003(6)
O(5)	0.076(9)	− 0.002(8)	− 0.006(9)	0.047(9)	− 0.019(9)	− 0.005(9)	0.004(9)
O(6)	0.045(9)	0.018(8)	− 0.017(8)	0.030(8)	− 0.031(8)	− 0.009(8)	− 0.064(8)
C(1)	0.45(2)	− 0.004(13)	0.048(15)	0.31(2)	0.015(14)	− 0.016(14)	0.026(14)
C(2)	0.38(2)	0.037(14)	− 0.020(15)	0.307(19)	0.048(13)	0.003(13)	− 0.014(12)
H(1)	0	0	0	0	0	0	0
H(2)	0	0	0	0	0	0	0
H(5A)	0	0	0	0	0	0	0
H(5B)	0	0	0	0	0	0	0
H(6A)	0	0	0	0	0	0	0
H(6B)	0	0	0	0	0	0	0

Table SI17: Refined octupole populations. If a parameter was not refined it is given a population of 0.

5.7 Hexadecapole Populations

	$P_{40}\,[\#e]$	$P_{41}\,[\#e]$	$P_{4-1}\,[\#e]$	$P_{42}\,[\#e]$	$P_{4-2}\,[\#e]$	$P_{43}\,[\#e]$	$P_{4-3}\,[\#e]$	$P_{44}\,[\#e]$	$P_{4-4}\,[\#e]$
Co(1)	−0.080(4)	0.047(4)	−0.033(4)	0.005(4)	0.045(4)	−0.033(3)	0.061(4)	−0.078(3)	−0.019(4)
Co(2)	−0.102(4)	−0.010(4)	0.030(4)	0.087(4)	0.018(4)	−0.072(4)	−0.051(4)	−0.073(4)	0.000(4)
O(1)	0	0	0	0	0	0	0	0	0
O(2)	0	0	0	0	0	0	0	0	0
O(3)	0	0	0	0	0	0	0	0	0
O(4)	0	0	0	0	0	0	0	0	0
O(5)	0	0	0	0	0	0	0	0	0
O(6)	0	0	0	0	0	0	0	0	0
C(1)	0	0	0	0	0	0	0	0	0
C(2)	0	0	0	0	0	0	0	0	0
H(1)	0	0	0	0	0	0	0	0	0
H(2)	0	0	0	0	0	0	0	0	0
H(5A)	0	0	0	0	0	0	0	0	0
H(5B)	0	0	0	0	0	0	0	0	0
H(6A)	0	0	0	0	0	0	0	0	0
H(6B)	0	0	0	0	0	0	0	0	0

Table SI18: Refined hexadecapole populations. If a parameter was not refined it is given a population of 0.

6 HIGH RESOLUTION MODEL PARAMETERS

6.1 Fractional coordinates

	x	y	z
Co(1)	0	0	0
Co(2)	0.5	0.5	0
O(1)	0.209586(16)	0.15649(2)	0.000168(17)
O(2)	0.437166(17)	0.22255(2)	−0.078063(18)
O(3)	0.096918(17)	−0.10148(2)	0.203110(15)
O(4)	0.089479(17)	−0.22899(2)	−0.097386(15)
O(5)	0.411016(18)	0.61025(3)	−0.197069(17)

O(6)	0.721055(17)	0.47746(2)	− 0.073824(17)
C(1)	0.324965(18)	0.11459(2)	− 0.063868(18)
C(2)	0.033753(18)	− 0.27976(2)	− 0.223423(17)
H(1)	0.3245(12)	− 0.027(2)	− 0.1098(12)
H(2)	− 0.071(2)	− 0.2166(16)	− 0.2714(12)
H(5A)	0.311(3)	0.5978(12)	− 0.2340(13)
H(5B)	0.4627(18)	0.6476(15)	− 0.270(2)
H(6A)	0.784(2)	0.398(3)	− 0.023(2)
H(6B)	0.7609(18)	0.589(4)	− 0.0549(12)

Table SI19: Refined atomic coordinates given in fractions of the unit cell vectors.

6.2 Thermal Parameters

	U^{11} [Å^2]	U^{22} [Å^2]	U^{33} [Å^2]	U^{12} [Å^2]	U^{13} [Å^2]	U^{23} [Å^2]
CO(1)	0.003079(9)	0.003121(11)	0.002918(9)	0.000001(6)	0.000309(6)	− 0.000016(6)
CO(2)	0.003113(9)	0.003847(12)	0.003769(10)	− 0.000129(7)	0.000447(7)	0.000116(7)
O(1)	0.00500(3)	0.00628(4)	0.00774(4)	− 0.00099(3)	0.00201(3)	− 0.00057(3)
O(2)	0.00570(3)	0.00643(4)	0.00936(4)	− 0.00161(3)	0.00293(3)	− 0.00177(3)
O(3)	0.00610(3)	0.00661(4)	0.00531(3)	− 0.00076(3)	0.00023(3)	0.00183(3)
O(4)	0.00648(3)	0.00618(4)	0.00515(3)	0.00126(3)	− 0.00008(3)	− 0.00167(2)
O(5)	0.00576(3)	0.01352(5)	0.00670(4)	0.00001(3)	0.00040(3)	0.00343(3)
O(6)	0.00558(3)	0.00647(4)	0.00817(4)	0.00031(3)	0.00122(3)	0.00000(3)
C(1)	0.00513(4)	0.00539(4)	0.00834(4)	− 0.00089(3)	0.00205(3)	− 0.00119(3)
C(2)	0.00610(4)	0.00615(4)	0.00588(4)	0.00138(3)	− 0.00070(3)	− 0.00194(3)
H(1)	0.021395	0.01312	0.027719	− 0.002103	0.00799	− 0.009637
H(2)	0.014063	0.018048	0.016777	0.002489	− 0.001842	0.001026
H(5A)	0.01102	0.026256	0.019576	− 0.005345	− 0.003135	0.002164
H(5B)	0.019015	0.029053	0.014334	− 0.007137	0.004822	0.004598
H(6A)	0.016427	0.015844	0.025511	0.003992	0.000527	0.003348
H(6B)	0.017813	0.012865	0.023218	− 0.003682	0.001338	0.00011

Table SI20: Refined ADPs of the atoms. No uncertainty on H ADPs as these are locked to the ones derived from SHADE3.

6.3 Monopole Population & Shielding Constants

	P_0 [#e]	κ	κ'
Co(1)	3.510(17)	1.046(4)	1
Co(2)	3.523(17)	1.050(4)	1
O(1)	6.38(2)	0.9852(13)	1.01(2)
O(2)	6.31(2)	0.9852(13)	1.01(2)
O(3)	6.34(2)	0.9852(13)	1.01(2)
O(4)	6.40(2)	0.9852(13)	1.01(2)
O(5)	6.23(4)	0.992(2)	0.87(2)
O(6)	6.29(4)	0.992(2)	0.87(2)
C(1)	4.13(5)	0.993(5)	0.919(15)
C(2)	4.06(5)	0.993(5)	0.919(15)
H(1)	1.01(3)	1.1	1.18
H(2)	1.00(3)	1.1	1.18
H(5A)	0.97(3)	1.18	1.5
H(5B)	0.95(3)	1.18	1.5
H(6A)	0.95(3)	1.18	1.5
H(6B)	0.95(3)	1.18	1.5

Table SI21: Refined monopole populations and shielding constants (κ and κ'). For H the shielding constants are locked to the midpoint of observed values. These values depend on what atom H is bonded to and they are based on modelling theoretical densities[18].

6.4 Dipole Populations

	P_{11} [#e]	P_{1-1} [#e]	P_{10} [#e]
Co(1)	0	0	0
Co(2)	0	0	0
O(1)	0.014(6)	− 0.000(6)	− 0.068(7)
O(2)	0.004(6)	0.001(6)	− 0.107(8)
O(3)	0.064(7)	− 0.001(7)	0.040(7)
O(4)	0.018(6)	0.014(6)	− 0.084(7)
O(5)	0.002(9)	− 0.027(12)	0.116(11)
O(6)	0.086(11)	− 0.074(12)	0.039(9)
C(1)	− 0.007(12)	− 0.008(13)	− 0.049(15)

C(2)	− 0.008(12)	0.010(13)	− 0.011(15)
H(1)	0	0	0.18(2)
H(2)	0	0	0.13(3)
H(5A)	0	0	0.11(3)
H(5B)	0	0	0.12(2)
H(6A)	0	0	0.09(3)
H(6B)	0	0	0.05(3)

Table SI22: Refined dipole populations. If a parameter was not refined it is given a population of 0.

6.5 Quadrupole Populations

	P_{20} [#e]	P_{21} [#e]	P_{2-1} [#e]	P_{22} [#e]	P_{2-2} [#e]
Co(1)	− 0.080(4)	0.004(5)	0.044(5)	− 0.121(4)	0.101(5)
Co(2)	− 0.068(5)	0.014(4)	0.095(5)	− 0.074(5)	− 0.049(5)
O(1)	− 0.062(7)	− 0.031(6)	0.019(6)	− 0.025(6)	− 0.037(6)
O(2)	− 0.047(6)	− 0.008(6)	− 0.000(6)	− 0.027(6)	0.039(6)
O(3)	0.062(6)	− 0.035(6)	0.059(6)	− 0.034(6)	− 0.039(6)
O(4)	0.023(6)	− 0.039(6)	0.002(6)	− 0.057(6)	0.010(6)
O(5)	0.028(8)	0.004(8)	0.016(9)	0.120(10)	− 0.044(8)
O(6)	0.006(8)	− 0.050(8)	0.087(8)	− 0.002(8)	− 0.083(9)
C(1)	0.092(12)	0.063(10)	0.012(11)	− 0.220(14)	− 0.001(10)
C(2)	0.085(13)	− 0.030(10)	− 0.046(11)	− 0.309(15)	0.032(10)
H(1)	0	0	0	0	0
H(2)	0	0	0	0	0
H(5A)	0.077(16)	0	0	0	0
H(5B)	0.103(18)	0	0	0	0
H(6A)	0.053(18)	0	0	0	0
H(6B)	0.086(17)	0	0	0	0

Table SI23: Refined quadrupole populations. If a parameter was not refined it is given a population of 0.

6.6 Octupole Populations

	P_{30} [#e]	P_{31} [#e]	P_{3-1} [#e]	P_{32} [#e]	P_{3-2} [#e]	P_{33} [#e]	P_{3-3} [#e]
Co(1)	0	0	0	0	0	0	0
Co(2)	0	0	0	0	0	0	0
O(1)	0.031(7)	− 0.000(6)	0.012(6)	0.012(6)	0.004(6)	− 0.008(6)	− 0.015(6)
O(2)	0.036(7)	0.003(6)	0.005(6)	0.010(6)	0.005(6)	− 0.002(6)	− 0.006(6)
O(3)	0.052(7)	− 0.008(6)	− 0.019(6)	0.004(6)	0.037(6)	− 0.014(6)	− 0.005(6)
O(4)	0.060(7)	0.011(6)	0.003(6)	0.021(6)	− 0.014(6)	0.011(6)	0.004(6)
O(5)	0.075(9)	− 0.001(8)	− 0.005(9)	0.046(9)	− 0.019(9)	− 0.005(9)	0.003(9)
O(6)	0.045(9)	0.019(8)	− 0.016(8)	0.031(8)	− 0.029(8)	− 0.010(8)	− 0.064(8)
C(1)	0.44(2)	− 0.005(13)	0.041(15)	0.30(2)	0.017(14)	− 0.016(13)	0.022(13)
C(2)	0.37(2)	0.037(14)	− 0.020(15)	0.297(19)	0.047(13)	0.006(13)	− 0.014(12)
H(1)	0	0	0	0	0	0	0
H(2)	0	0	0	0	0	0	0
H(5A)	0	0	0	0	0	0	0
H(5B)	0	0	0	0	0	0	0
H(6A)	0	0	0	0	0	0	0
H(6B)	0	0	0	0	0	0	0

Table SI24: Refined octupole populations. If a parameter was not refined it is given a population of 0.

6.7 Hexadecapole Populations

	P_{40} [#e]	P_{41} [#e]	P_{4-1} [#e]	P_{42} [#e]	P_{4-2} [#e]	P_{43} [#e]	P_{4-3} [#e]	P_{44} [#e]	P_{4-4} [#e]
Co(1)	-0.081(4)	0.045(4)	-0.033(4)	0.009(4)	0.045(4)	-0.035(3)	0.060(4)	-0.077(3)	-0.019(4)
Co(2)	-0.101(4)	-0.010(4)	0.030(4)	0.085(4)	0.018(4)	-0.071(4)	-0.051(4)	-0.069(4)	0.000(4)
O(1)	0	0	0	0	0	0	0	0	0
O(2)	0	0	0	0	0	0	0	0	0
O(3)	0	0	0	0	0	0	0	0	0
O(4)	0	0	0	0	0	0	0	0	0
O(5)	0	0	0	0	0	0	0	0	0
O(6)	0	0	0	0	0	0	0	0	0
C(1)	0	0	0	0	0	0	0	0	0
C(2)	0	0	0	0	0	0	0	0	0

H(1)	0	0	0	0	0	0	0	0	0
H(2)	0	0	0	0	0	0	0	0	0
H(5A)	0	0	0	0	0	0	0	0	0
H(5B)	0	0	0	0	0	0	0	0	0
H(6A)	0	0	0	0	0	0	0	0	0
H(6B)	0	0	0	0	0	0	0	0	0

Table SI25: Refined hexadecapole populations. If a parameter was not refined it is given a population of 0.

7 ANHARMONIC MODEL PARAMETERS

7.1 Fractional coordinates

	x	y	z
Co(1)	0	0	0
Co(2)	0.5	0.5	0
O(1)	0.209582(16)	0.15649(2)	0.000172(16)
O(2)	0.437170(17)	0.22255(2)	−0.078066(17)
O(3)	0.096919(16)	−0.10149(2)	0.203110(15)
O(4)	0.089478(16)	−0.228991(19)	−0.097384(15)
O(5)	0.411024(17)	0.61025(3)	−0.197069(17)
O(6)	0.721047(16)	0.47746(2)	−0.073826(16)
C(1)	0.324965(17)	0.11460(2)	−0.063868(17)
C(2)	0.033756(18)	−0.27976(2)	−0.223425(16)
H(1)	0.3244(12)	−0.027(2)	−0.1094(12)
H(2)	−0.0724(19)	−0.2162(15)	−0.2713(12)
H(5A)	0.308(3)	0.5973(11)	−0.2349(12)
H(5B)	0.4646(16)	0.6484(14)	−0.2721(19)
H(6A)	0.784(2)	0.398(3)	−0.0235(18)
H(6B)	0.7614(16)	0.592(4)	−0.0545(12)

Table SI26: Refined atomic coordinates given in fractions of the unit cell vectors.

7.2 2nd Order Gram-Charlier Parameters

	U^{11} [Å^2]	U^{22} [Å^2]	U^{33} [Å^2]	U^{12} [Å^2]	U^{13} [Å^2]	U^{23} [Å^2]
Co(1)	0.00331(5)	0.00255(5)	0.00303(5)	0.00001(3)	0.00044(4)	-0.00001(3)
Co(2)	0.00326(5)	0.00324(5)	0.00387(5)	-0.00008(3)	0.00050(4)	0.00009(3)
O(1)	0.00495(3)	0.00622(4)	0.00771(4)	-0.00098(3)	0.00202(3)	-0.00057(3)
O(2)	0.00566(3)	0.00634(4)	0.00935(4)	-0.00160(3)	0.00293(3)	-0.00177(3)
O(3)	0.00609(3)	0.00650(4)	0.00529(3)	-0.00075(3)	0.00026(3)	0.00183(3)
O(4)	0.00643(3)	0.00611(4)	0.00512(3)	0.00124(3)	-0.00008(3)	-0.00166(2)
O(5)	0.00573(4)	0.01343(5)	0.00667(4)	0.00001(3)	0.00040(3)	0.00344(3)
O(6)	0.00553(3)	0.00641(4)	0.00814(4)	0.00030(3)	0.00122(3)	-0.00000(3)
C(1)	0.00507(4)	0.00532(4)	0.00829(4)	-0.00089(3)	0.00205(3)	-0.00119(3)
C(2)	0.00606(4)	0.00607(4)	0.00583(4)	0.00138(3)	-0.00069(3)	-0.00194(3)
H(1)	0.022709	0.014324	0.027758	-0.001768	0.007524	-0.008884
H(2)	0.013648	0.018877	0.017516	0.004144	-0.001278	0.001618
H(5A)	0.011414	0.027203	0.021616	-0.004046	-0.001731	0.002539
H(5B)	0.018699	0.029596	0.01711	-0.005265	0.005642	0.005496
H(6A)	0.017899	0.015834	0.023713	0.004721	0.00059	0.003184
H(6B)	0.018964	0.013113	0.0243	-0.002688	0.001619	0.000707

Table SI27: Refined 2nd order Gram-Charlier parameters (equivalent to anisotropic ADPs) of the atoms. No uncertainty on H ADPs as these are locked to the ones derived from SHADE3.

7.3 4th Order Gram-Charlier Parameters

	Co(1)	Co(2)
δ^{1111}	$2.1(4) \times 10^{-9}$	$1.3(4) \times 10^{-9}$
δ^{2222}	$-1.00(10) \times 10^{-8}$	$-9.9(10) \times 10^{-8}$
δ^{3333}	$9(3) \times 10^{-10}$	$7(3) \times 10^{-10}$
δ^{1112}	$-1(2) \times 10^{-10}$	$3(2) \times 10^{-10}$
δ^{12222}	$4(3) \times 10^{-10}$	$6(3) \times 10^{-10}$
δ^{1113}	$3(2) \times 10^{-10}$	$0(2) \times 10^{-10}$
δ^{1333}	$6(2) \times 10^{-10}$	$3(2) \times 10^{-10}$
δ^{2223}	$0(3) \times 10^{-10}$	$1(3) \times 10^{-10}$
δ^{2333}	$0(2) \times 10^{-10}$	$-3(2) \times 10^{-10}$
δ^{1122}	$0(2) \times 10^{-10}$	$-7(2) \times 10^{-10}$
δ^{1133}	$3(1) \times 10^{-10}$	$3(1) \times 10^{-10}$

δ^{2233}	$-3(1)\times10^{-10}$	$-5(1)\times10^{-10}$
δ^{1123}	$0(1)\times10^{-10}$	$-1(1)\times10^{-10}$
δ^{1223}	$2(1)\times10^{-10}$	$0(1)\times1^{-10}$
δ^{1233}	$-1(1)\times10^{-10}$	$-1(1)\times10^{-10}$

Table SI28: Refined 4th order Gram-Charlier parameters of the transition metals.

7.4 Monopole Population & Shielding Constants

	P_0 [#e]	κ	κ'
Co(1)	3.57(2)	1.047(4)	1
Co(2)	3.594(19)	1.047(4)	1
O(1)	6.36(2)	0.9906(14)	0.99(2)
O(2)	6.28(2)	0.9906(14)	0.99(2)
O(3)	6.33(2)	0.9906(14)	0.99(2)
O(4)	6.37(2)	0.9906(14)	0.99(2)
O(5)	6.19(4)	0.999(2)	0.86(2)
O(6)	6.25(4)	0.999(2)	0.86(2)
C(1)	4.12(5)	0.997(5)	0.903(14)
C(2)	4.06(5)	0.997(5)	0.903(14)
H(1)	1.03(3)	1.1	1.18
H(2)	0.99(3)	1.1	1.18
H(5A)	0.97(3)	1.18	1.5
H(5B)	0.95(3)	1.18	1.5
H(6A)	0.97(3)	1.18	1.5
H(6B)	0.97(3)	1.18	1.5

Table SI29: Refined monopole populations and shielding constants (κ and κ'). For H the shielding constants are locked to the midpoint of observed values. These values depend on what atom H is bonded to and they are based on modelling theoretical densities[18].

7.5 Dipole Populations

	P_{11} [#e]	P_{1-1} [#e]	P_{10} [#e]
Co(1)	0	0	0
Co(2)	0	0	0
O(1)	0.015(6)	0.001(6)	−0.071(7)
O(2)	0.004(6)	−0.001(6)	−0.109(8)

O(3)	0.066(7)	− 0.003(7)	0.044(7)
O(4)	0.017(6)	0.014(6)	− 0.088(7)
O(5)	0.001(9)	− 0.026(12)	0.123(11)
O(6)	0.092(11)	− 0.076(12)	0.035(9)
C(1)	− 0.007(12)	− 0.012(13)	− 0.059(15)
C(2)	− 0.008(12)	0.005(13)	− 0.010(16)
H(1)	0	0	0.20(2)
H(2)	0	0	0.15(3)
H(5A)	0	0	0.15(2)
H(5B)	0	0	0.16(2)
H(6A)	0	0	0.10(3)
H(6B)	0	0	0.08(3)

Table SI30: Refined dipole populations. If a parameter was not refined it is given a population of 0.

7.6 Quadrupole Populations

	P_{20} [#e]	P_{21} [#e]	P_{2-1} [#e]	P_{22} [#e]	P_{2-2} [#e]
Co(1)	− 0.096(8)	0.066(9)	− 0.020(9)	− 0.072(8)	0.063(8)
Co(2)	0.012(9)	− 0.019(7)	0.029(9)	− 0.077(10)	− 0.056(9)
O(1)	− 0.063(7)	− 0.030(6)	0.022(6)	− 0.027(6)	− 0.035(6)
O(2)	− 0.049(7)	− 0.010(6)	0.005(6)	− 0.030(6)	0.036(6)
O(3)	0.059(6)	− 0.032(6)	0.056(6)	− 0.042(6)	− 0.037(6)
O(4)	0.021(6)	− 0.039(6)	− 0.001(6)	− 0.056(6)	0.007(6)
O(5)	0.028(8)	− 0.003(8)	0.021(9)	0.133(10)	− 0.051(8)
O(6)	0.009(8)	− 0.053(8)	0.090(9)	0.002(8)	− 0.084(9)
C(1)	0.096(12)	0.063(11)	0.008(11)	− 0.238(15)	− 0.002(10)
C(2)	0.082(13)	− 0.035(10)	− 0.041(11)	− 0.331(16)	0.029(11)
H(1)	0	0	0	0	0
H(2)	0	0	0	0	0
H(5A)	0.091(16)	0	0	0	0
H(5B)	0.127(19)	0	0	0	0

H(6A)	0.058(18)	0	0	0	0
H(6B)	0.099(18)	0	0	0	0

Table SI31: Refined quadrupole populations. If a parameter was not refined it is given a population of 0.

7.7 Octupole Populations

	P_{30} [#e]	P_{31} [#e]	P_{3-1} [#e]	P_{32} [#e]	P_{3-2} [#e]	P_{33} [#e]	P_{3-3} [#e]
Co(1)	0	0	0	0	0	0	0
Co(2)	0	0	0	0	0	0	0
O(1)	0.031(6)	− 0.000(6)	0.011(6)	0.013(6)	0.004(6)	− 0.007(6)	− 0.016(6)
O(2)	0.036(6)	0.005(6)	0.004(6)	0.009(6)	0.006(6)	− 0.002(6)	− 0.006(6)
O(3)	0.053(7)	− 0.009(6)	− 0.021(6)	0.005(6)	0.037(6)	− 0.015(6)	− 0.005(6)
O(4)	0.062(7)	0.013(6)	0.004(6)	0.021(6)	− 0.014(6)	0.012(6)	0.004(6)
O(5)	0.076(9)	− 0.002(8)	− 0.006(9)	0.048(9)	− 0.016(9)	− 0.004(9)	0.004(9)
O(6)	0.045(9)	0.019(8)	− 0.017(8)	0.030(8)	− 0.032(8)	− 0.009(8)	− 0.064(8)
C(1)	0.46(3)	− 0.001(13)	0.051(15)	0.32(2)	0.012(14)	− 0.019(14)	0.028(14)
C(2)	0.39(2)	0.038(14)	− 0.023(15)	0.31(2)	0.050(13)	0.001(13)	− 0.015(12)
H(1)	0	0	0	0	0	0	0
H(2)	0	0	0	0	0	0	0
H(5A)	0	0	0	0	0	0	0
H(5B)	0	0	0	0	0	0	0
H(6A)	0	0	0	0	0	0	0
H(6B)	0	0	0	0	0	0	0

Table SI32: Refined octupole populations. If a parameter was not refined it is given a population of 0.

7.8 Hexadecapole Populations

	P_{40} [#e]	P_{41} [#e]	P_{4-1} [#e]	P_{42} [#e]	P_{4-2} [#e]	P_{43} [#e]	P_{4-3} [#e]	P_{44} [#e]	P_{4-4} [#e]
Co(1)	− 0.091(6)	0.042(6)	− 0.025(6)	− 0.007(6)	0.043(6)	− 0.023(5)	0.041(6)	− 0.081(5)	− 0.022(6)
Co(2)	− 0.107(6)	− 0.010(6)	0.018(7)	0.081(6)	0.024(5)	− 0.077(6)	− 0.047(6)	− 0.087(6)	− 0.000(6)
O(1)	0	0	0	0	0	0	0	0	0
O(2)	0	0	0	0	0	0	0	0	0

O(3)	0	0	0	0	0	0	0	0	0
O(4)	0	0	0	0	0	0	0	0	0
O(5)	0	0	0	0	0	0	0	0	0
O(6)	0	0	0	0	0	0	0	0	0
C(1)	0	0	0	0	0	0	0	0	0
C(2)	0	0	0	0	0	0	0	0	0
H(1)	0	0	0	0	0	0	0	0	0
H(2)	0	0	0	0	0	0	0	0	0
H(5A)	0	0	0	0	0	0	0	0	0
H(5B)	0	0	0	0	0	0	0	0	0
H(6A)	0	0	0	0	0	0	0	0	0
H(6B)	0	0	0	0	0	0	0	0	0

Table SI33: Refined hexadecapole populations. If a parameter was not refined it is given a population of 0.

8 REFERENCES

1 F. Illas and R. L. Martin, *J. Chem. Phys.*, 1998, **108**, 2519–2527.

2 R. F. W. Bader, *Atoms in Molecules - A Quantum Theory*, Clarendon Press, Oxford, UK, 1994.

3 G. Ferraris and M. Franchini-Angela, *Acta Crystallogr. Sect. B Struct. Crystallogr. Cryst. Chem.*, 1972, **B28**, 3572–3583.

4 G. S. Chandler, M. Wajrak and R. N. Khan, *Acta Cryst.*, 2015, **B71**, 275–284.

5 G. Chiari and G. Ferraris, *Acta Cryst.*, 1982, **B38**, 2331–2341.

6 C. Gatti, *Z. Kristallogr.*, 2005, **220**, 399–457.

7 P. Macchi and A. Sironi, *Coord. Chem. Rev.*, 2003, **238**–**239**, 383–412.

8 R. Scatena, R. D. Johnson, P. Manuel and P. Macchi, *J. Mater. Chem. C*, 2020, **8**, 12840–12847.

9 P. L. Popelier, *Atoms in Molecules - An Introduction*, Peason Education Limited, Harlow, UK, 2000.

10 C. Gatti, F. Cargnoni and L. Bertini, *J. Comput. Chem.*, 2003, **24**, 422–436.

11 R. Kamiński, S. Domagała, K. N. Jarzembska, A. A. Hoser, W. F. Sanjuan-Szklarz, M. J. Gutmann, A. Makal, M. Malińska, J. M. Bąk and K. Woźniak, *Acta Cryst.*, 2014, **A70**, 72–91.

12 L. Krause, B. Niepötter, C. J. Schürmann, D. Stalke and R. Herbst-Irmer, *IUCrJ*, 2017, **4**, 420–430.

13 Y. A. Abramov, *Acta Cryst.*, 1997, **A53**, 264–272.

14 J. R. Sabino and P. Coppens, *Acta Cryst.*, 2003, **A59**, 127–131.

15 A. Volkov, P. Macchi, L. J. Farrugia, C. Gatti, P. R. Mallinson, T. Richter and T. Koritsanszky, *XD2016 - A Computer Program Package for Multipole Refinement, Topological Analysis of Charge Densities and Evaluation of Intermolecular Energies from Experimental or Theoretical Structure Factors*, 2016.

16 R. Herbst-Irmer, J. Henn, J. J. Holstein, C. B. Hübschle, B. Dittrich, D. Stern, D. Kratzert and D. Stalke, *J. Phys. Chem. A*, 2013, **117**, 633–641.

17 A. Holladay, P. Leung and P. Coppens, *Acta Cryst.*, 1983, **A39**, 377–387.

18 A. Volkov, Y. A. Abramov and P. Coppens, *Acta Cryst.*, 2001, **A57**, 272–282.